

Enhancement of thermal power plant performance through solar-assisted feed water heaters: An innovative repowering approach



Sifat Abdul Bari, Mohtasim Fuad, Kazi Fahad Labib, M. Monjurul Ehsan*, Yasin Khan, Muhammad Mahmood Hasan

Department of Mechanical and Production Engineering (MPE), Islamic University of Technology (IUT), Board Bazar, Gazipur 1704, Bangladesh

ARTICLE INFO

Keywords:
 Steam power plant
 Rankine Cycle
 Feed Water Heaters
 Solar Energy
 Parabolic Trough Collector
 Thermal Analysis

ABSTRACT

Increasing the efficiency of a power plant by optimization or repowering has always been a crucial challenge for energy analysts. At the same time as natural energy resources are limited, the integration of renewable energy sources such as solar energy has been prioritized for the past few decades. This study presents a way of enhancing a thermal power plant with a regenerative reheating Rankine cycle, evaluating the impact of solar-powered heat exchangers on feed water heating at 200 MW single unit of the Shahid Montazeri Power Plant operating at 13 MPa and 540 °C. Increases in energy-exergy efficiencies, power output and fuel save due to this modification have been studied in 14 different cases which have been analyzed in Engineering Equation Solver (EES). The case studies cover replacing single, double, and triple Feed Water Heaters (FWH). Parametric analysis of the four most promising cases has been performed in varying operating conditions such as main steam and reheat steam temperature and pressure and condensation pressure. In the most favorable configuration (case 12), the net thermal power output increases to 225 MW while energy and exergy efficiency increases to 39.73 % and 43.99 % respectively. Exergy and energy loss across different major components have been presented as well which indicates room for further improvement and contributes valuable insights to thermal power plant optimization for sustainable and efficient energy solutions in the future.

1. Introduction

Most of the developing nations are heavily dependent upon utilizing fossil fuels for power generation which made up to 82 % of the global energy consumptions [1]. This is projected to rise further as reported by the International Energy Agency. Extensive researches have been conducted to study the adverse effects and consequences if it continues [2–5]. Steam power plants produce a large amount of electricity worldwide. It's evident to adapt to more efficient power generation processes or incorporate renewable energy sources with existing systems. It's a ray of hope that Over 130 nations, including the European Union, have agreed to collaborate on tripling global renewable energy capacity to at least 11,000 GW by 2030. [6].

Modifications on the existing cycle such as reheating and regeneration increase the efficiency of traditional Rankine cycle which is used in most of the coal and natural gas utilized power plants [7–9]. Preheating water through Feed Water Heaters (FWHs) raises the temperature and reduces the irreversibly during steam generation to some margin which

leads to lower energy usage improving the overall efficiency [10–12]. Optimizing FWH number and placement maximizes cycle efficiency even further [13,14]. Specific arrangements like using a combined cycle, Heat Recovery Steam Generators (HRSG), cogeneration plants result in increased performance [15–18]. Appropriate boiler, condenser sizing and operating conditions leads to less energy and exergy losses [19–21]. Studies conducted by Lei Tan and Ahmed M. Daabo to increase the performance of different turbomachinery of power plant such as pumps and turbines are widely acknowledged [22–25].

Even after this much advancement, integration of solar energy is very intriguing as the available solar resources on Earth exceed the present world's energy demand by several hundred times. Concentrated Solar Power (CSP) can play an important role in locations with abundant solar resources [26–28]. To reduce the load on natural resources and at the same time to increase the performance of the power plant, integration of renewable energy resources such as Concentrated Solar Power (CSP) technologies is being studied widely in recent times. This method concentrates direct solar radiation to produce high-temperature thermal energy, which is transformed into electricity via a thermodynamic cycle

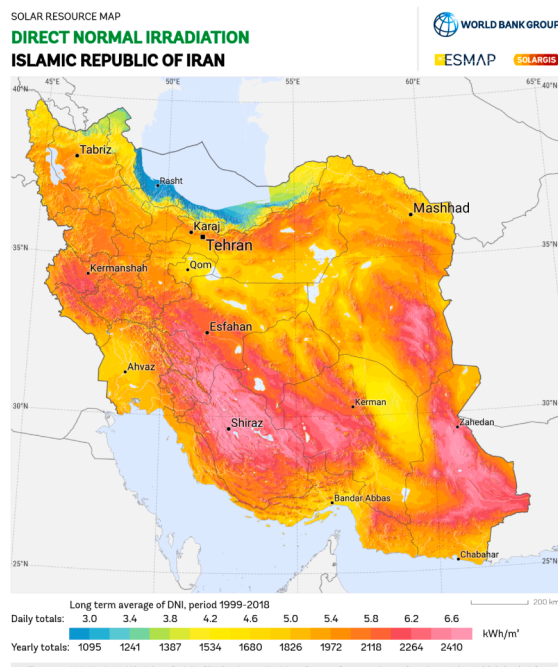
* Corresponding author.

E-mail address: ehsan@iut-dhaka.edu (M. Monjurul Ehsan).

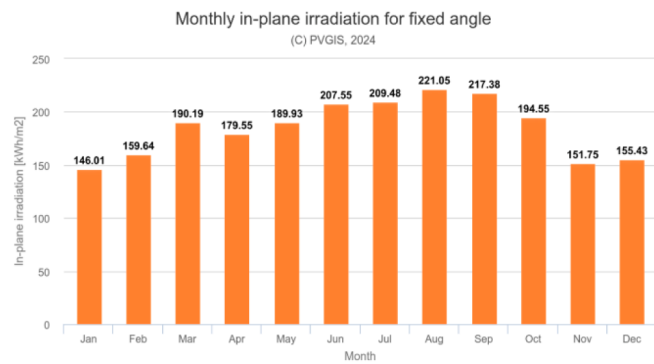
Nomenclature		Abbreviations
\dot{m}	Mass flow rate, kg/s	B_f Energy consumption by boiler without repowering
\dot{Q}	Rate of heat, kW	B_f^R Energy consumption by boiler with repowering
\dot{W}	Rate of work, kW	
h	Specific enthalpy, kJ/kg	
h_0	Specific enthalpy at atmospheric temperature and pressure, kJ/kg	
s	Specific entropy, kJ/kg-K	
s_0	Specific entropy at atmospheric temperature and pressure, kJ/kg-K	
ψ	Specific flow exergy, kJ/kg	
\dot{E}_x	Total flow exergy rate, kW	
T_0	Atmospheric temperature, K	CSP Concentrated Solar Power
T	Temperature, K	LCOE levelized cost of energy
$\dot{i}_{\text{destroyed}}$	Rate of destroyed exergy, kW	PV Photovoltaic
\dot{Q}_l	Rate of heat loss, kW	CP Condensate Pump
η_1	1st law efficiency	WCP Water Circulating Pump
η_2	2nd law efficiency	HPT High Pressure Turbine
P	Pressure, MPa	IPT Intermediate Pressure Turbine
P_0	Atmospheric pressure, MPa	LPT Low-Pressure Turbine
\dot{X}_{ch}	Chemical Exergy Rate, kW	HPH High-Pressure Heater
A_c	Solar Collector Area	LPH Low-Pressure Heater
Q_s	Heat input required for the feed water heater by solar farm	PTC Parabolic Trough Collector
N_e	Net electric power output	FWH Feed Water Heater
Q_b^R	Total heat input to boiler after repowering	LFR Linear Fresnel Collector
Q_b	Total heat input to boiler without repowering	EXV Expansion Valve
		BFP Feed Pump – Boiler
		CT Cooling Tower
Subscripts		
	i	Inlet
	o	Outlet
	De	Deaerator
	c	Condenser
	b	Boiler

using an electric generator. CSP integrated power plants which is the focus of this study, have been investigated over the last three decades due to its appealing prospective. Boiler air preheating, along with steam superheating and steam reheating are some of the most researched procedures to combine solar power with existing power plants. [29–31].

Parabolic Trough Collector (PTC) is a specific solar concentrating technique that is capable of heating the working fluid in a large-scale power plant as it's a suitable option for application in the temperature range of 400–450 °C [27,32]. Compared to solar tower-based plants, these designs are simpler and characterized by substantially cheaper



(a)



Slope angle: 35°

Azimuth angle: 0°

Yearly in-plane irradiation: 2222.5 kWh/m²

(b)

Fig. 1. Solar irradiance properties a) Direct Normal Irradiation, b) Monthly In-Plane irradiation properties, in Iran.

investments, as PTC are less expensive.

The prospects of combining renewable energy source such as CSP in Shahid Montazeri power plant located in Isfahan, Iran (Coordinates $32^{\circ}47'42.29''N$, $51^{\circ}30'18.22''E$) has been investigated in this study. The Power plant is composed of a total of 8 units each capable of generating 200 MW, in total 1600 MW per hour. As suggested by numerous studies, Iran is one of the best places to construct solar power plants and solar repowering facilities [33–35]. Fig. 1(a) shows the direct normal irradiance (DNI) throughout Iran as modeled by the SolarGIS satellite solar resource model [36]. Investigated power plant location Isfahan, receives a high direct irradiance in range of 5.80 to 6 kWh/m² daily making it a suitable location for CSP system. Fig. 1(b) illustrates monthly in plane irradiance (kWh/m²) of Isfahan obtained from the European Union PV-GIS website simulation. With an average yearly irradiance of over 2000 kWh/m², the Prospects of CSP system in Isfahan, Iran is very promising [37,38]. Significant investigations on repowering power plant with CSP-PTC technology have been carried out in many different power generation facilities worldwide in recent times to study the prospects and Potentials.

Erkinjon and Zarina [39] studied the effectiveness of replacing regenerative FWHs, economizer and repowering steam generator with PTC having 197.5 m length, 5.76 m aperture width and 1.71 m focal length in a 155 MW steam power plant in Tashkent. Simulation results showed that solar to electric efficiency increased with higher temperature of solar heat input. Replacing High Pressure Heater (HPH) demonstrated an efficiency of 0.270, which was higher than putting low repressure FWH, which yielded 0.078. Highest operating temperature of PTC was recorded to be 393 °C at an average direct normal irradiance of 847 W/m². Hisham et al. [40] investigated the potential of CSP-PV integrated hybrid solar power plant in two cities of Saudi Arabia upon studying the direct normal irradiance (DNI) and global horizontal irradiance (GHI) throughout Saudi Arabia as modeled by the SolarGIS satellite solar resource mode. The simulation work done using NREL System Advisor Model (SAM) model showed that for the 50 MW CSP-PTC standalone plant with a target capacity of 79 % required solar multiple for the solar collector field was 6 for Riyadh city and 3.5 for Tabuk city. Obtained results were later linked with an economic model which calculated the leveled cost of energy (LCOE) for Riyadh to be 0.177 \$/kWh and 0.137 \$/kWh for Tabuk city.

Md. Ibthisum Alam et al. [41] presented the prospects of CSP technologies reviewing several studies from past two decades. The study showed PTC to be capable of generating more than 100 MW unit power with an integrated thermal storage system upon reviewing different existing power generating facilities. The study showed that PTC can be utilized in operating temperature range of 250–550 °C with peak efficiency over 20 % and there are already several operational PTC integrated CSP facilities producing power in USA, Morocco and Israel while 3 units of 200 MW PTC plant is under construction in UAE. Jessica Settino et al. [42] evaluated integration of CSP-PTC technology with the topping gas turbine cycle of a combined power plant. The overall cycle with PTC to operate in a temperature range up to 600 °C has been simulated in Thermoflex™ with 800 W/m² DNI of solar field to preheat the air before entering combustion chamber. The study showed efficiency of solar conversions and electric system to be 33 % and 69.5 % respectively in one stage intercooling configuration. A one-year simulation was conducted in Messina and Torino, two cities with distinct climates, to test this setup under real-world operational conditions which showed that both towns may reach an average yearly solar-to-electric efficiency of roughly 32 %, resulting in natural gas savings of 7.7 % and 5.8 %, respectively. The energy analysis of the overall cycle was performed. However, exergy analysis or component wise study had not been included. Any modifications in bottoming cycle had not been addressed as well.

A study conducted by Omal J. Khaleel et al. [43] focused on the energy and exergy analysis of different thermal power plants and several

studies over the past few years were critically evaluated. It has been observed from numerous research that a major portion of exergy and energy is lost in the boiler and condenser respectively. Total exergy loss in boiler, condenser and turbine combined to approximately 84 % of the total exergy destruction. It appeared that increasing the average temperature at which heat is added to the working fluid is the best optimization to increase the efficiency of the power plant. The study also suggested different component wise improvements along with future work scopes such as detailed study on the effect on ambient temperature on the performance of the thermal power plant, developing complex code on analytical software, investigation of power plant performance in case of with and without FWHs and increasing the number of FWHs. Adam R. Jensen et al. [44] studied the performance of Bronderslev CSP-Biomass hybrid power plant operating at organic Rankine cycle. Solar collector field with 40 PTC led to an annual DNI of 1040 kWh/m². With the total aperture area of 26,930 m² highest recorded temperature on 16 MW PTC was 340°C. From the analysis the annual efficiency of the plant was obtained to be 93 % ensuing 61 % of the total heat demand of the city. Attached heat recovery system utilized wasted heat and resulted in lowering fuel consumption of 10.2 million m² compared to subsequent year.

Sorour Alotaibi et al. [45] examined the efficiency of Az-Zour South power plant in Kuwait, modified with a solar assisted regenerative system incorporating PTC during peak load conditions. The traditional 300 MW plant modeled with PTC was simulated at Kuwait's weather conditions according to the revised ASHRAE model for Middle East countries. For optimum PTC area of 25,850 m² with an annual solar irradiance of 2300 kWh/m²/y resulted in increased power generation of 9.8 MW which led to about 1.5 % cycle and thermal efficiency. LCOE study illustrated the cost per kWh power generation for each month of the year. In this study only two Low Pressure Heater (LPH) was replaced with CSP technology. The effect of replacing HPH or combination of HPH and LPH had not been discussed. Additionally, detailed exergy and energy analysis which would have shown effects on different component's performance and sources of irreversibility were not studied. S. Kabiri et al. [46] analyzed the effectiveness of repowering 320 MW unit of Bandar Abbas power plant in Iran with CSP-PTC integrated feed water heaters. Climate conditions were obtained from TRNSYS software which showed average DNI for each month of the year. The study investigated the prospects of utilizing both low pressure and high-pressure solar collectors assuming the condenser size to be increased by 45 %. Obtained results showed the maximum power output of 400 MW in the months of higher solar irradiance. Advanced exergy analysis showed that 10 % of the total exergy destruction is avoidable for the boiler and in the case of condenser unavoidable exergy destruction is about 87 % of the total destruction. Dynamic environmental and economic analysis revealed that the benefits in a 30-year period will be over \$90 million considering solar factor to be one.

Mehdi et al. [47] examined the performance of 250 MW natural gas fired power plant in Abyek, Qazvin, Iran by preheating the feed water up to 290 °C through PTC at the economizer inlet. The study was simulated in Thermoflow and MATLAB software. Highest temperature of 393 °C at the PTC was obtained by a solar field of 120,000 m² having an average irradiance of 1050 W/m². This arrangement led overall thermal efficiency to increase by 2.1 % and power generation to 24 MW. Economic and environmental analysis provided cost of energy generation to be 80\$/kWh and payback period of 6 years and reduction of fuel usage and CO₂ emission. Gholamreza Ahmadi et al. [29] investigated integration of solar energy in 320 MW unit of Isfahan steam power plant in Iran by replacing HPH with PTC farm. 7 different scenarios were simulated using Cycle Tempo software. The results showed that replacing all high-pressure feed water preheaters with solar farms increases the net energy and energy efficiencies of the power plant by 18.3 % compared to the simple cycle, which reach 45 % and 43.91 % respectively, for a 9-hour solar system operated with DNI and solar

collector efficiency of 500 W/m^2 and 60 %, respectively. Environmental and economic study had been conducted as well. However, case study with LPH or combining HPH and LPH, effect on different component performance were not addressed.

This study presents the prospect of FWHs that employ PTC technology to improve the efficiency of the thermal cycle. In this solar-thermal hybrid technology, FWHs are powered by PTC. This integration enables the system to operate with higher power output and energy utilization. The whole power plant model was simulated through code developed in EES software. In the case study simulation, different extractions were cut off and as a result, different turbines got more steam flow at the inlet which turned into greater energy output and efficiency. The novelty of the work lies in determining the most efficient configuration considering the number of FWHs that need to be repowered and other operating parameters. The exergy analysis presented a thorough assessment of energy quality and inefficiencies in the process of power generation, identifying specific areas that can be targeted for enhancement. With an increased mass flow rate the net unit output increases but so does the condenser pressure. The condenser output temperature increases. So, optimizing this suitable operating condition is an important design criterion of thermal power plants. Taking mass flow rate of the system as a practical design criterion, case studies were further scrutinized for parametric study. The parametric analysis investigated the effect of several parameters including temperature, pressure, and flow rates, to determine the optimal conditions for these plants.

The study focuses on sustainability through these modifications as it emphasizes diminishing greenhouse gas emissions and preserving resources. Fuel savings due to repowering in each case has been presented. The research creates a significant framework for enhancing the design and operation of power plants, effectively managing the trade-off between efficiency, sustainability, and cost-efficiency. This has enormous implications for both the energy sector and the preservation of the environment.

2. Power plant description

The Shahid Montazeri power plant operates a regenerative-reheat Rankine cycle as shown in Fig. 2.[48] Water from the condenser is pressurized by the condensate pump (CP), progressing through low-pressure heaters (LPH 1–4) and the deaerator the feed water temperature gradually increases. The deaerator serves as an open feedwater heater, enhancing water temperature further with extracted turbine steam. A feedwater pump then elevates the water pressure to the boiler's operating pressure. After passing through high-pressure heaters (HPH 5–7), the water enters the boiler, transforming into superheated vapor. Very high temperature and high work potential steam is directed to the High-Pressure Turbine (HPT) and is let to expand turning the shaft of the turbine to produce power. In this power plant cycle, 3 stages of turbines are used. Steam extraction from a high-pressure turbine is done in two stages at a pressure lower than the boiler pressure and it is used in HPH 7 and HPH 6 for heating the feed water heater. The rest of the steam extracted from the high-pressure turbine is sent to the superheater where it is heated again up to the maximum temperature of the cycle. When the steam leaves the superheater, it is directed to the Intermediate Pressure Turbine (IPT) and is let to expand generating work output from the turbine. Some steam is extracted from the intermediate pressure turbine at 5 stages and is used to heat the feed water heater in HPH-5, deaerator, LPH-4, LPH-3, and LPH-2. The rest of the steam is taken from the intermediate pressure turbine then enters the Low-Pressure Turbine (LPT) and is expanded generating work output from the turbine like before. Some steam is also extracted from the low-pressure turbine and is used in LPH-1 to heat the feed water heater. Steam leaves the low-pressure turbine as a saturated vapor-liquid mixture of the desired quality and enters the condenser for condensation or heat rejection to re-enter the cycle. The operating condition of this power plant is depicted in Table 1.

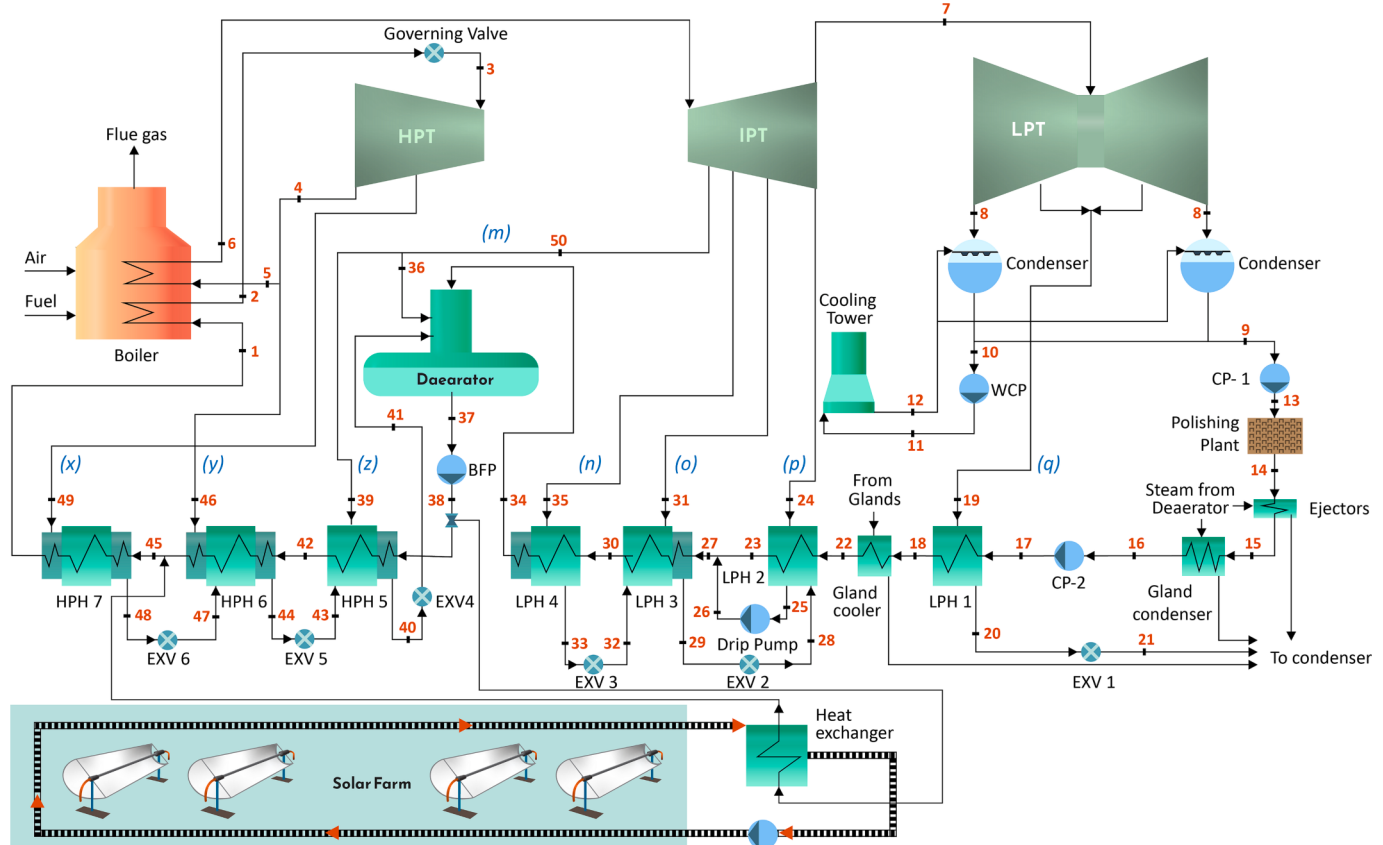


Fig. 2. Schematic Diagram of the regenerative reheat Rankine power plant with PTC-powered feed water heaters.

3. Research methodology

3.1. Assumptions

The following assumptions are taken to simplify the working principles and develop a numerical model of existing Shahid Montazeri powerplant studied by Ahmadi et. al [48].

- All the components have been working under steady-state conditions.
- When performing the exergy and energy analysis, some auxiliary equipment is deemed to have less of an impact on the power cycle and was therefore ignored.
- Auxiliary components between CP-1 and CP-2 are omitted during the analysis.
- Condensate Pump –1 and condensate pump are merged for simplification and replaced with one condensate pump having the input pressure of CP-1 as input and outlet pressure of CP-2 as output.
- During the mass balance analysis for extracted steam, the total mass flow rate of the working fluid is considered 1 kg/s, and calculations are performed on this basis.
- Ideal operating conditions are assumed during mass balance analysis of extracted steam. Thus, heat loss, pressure drop, and frictional loss are disregarded, and turbines and pumps are working under isentropic conditions.
- During the numerical analysis of the cycle, the components that are disregarded are – Gland Cooler, Gland Condenser, Ejector, Circulating Water Pump (CWP), Drip pump, and Cooling tower.
- For exergy analysis, pressure and temperature of surrounding conditions are taken as 101.3 kPa and 298.15 K respectively.

3.2. Workflow methodology

In this project, the exergy and energy analysis of the stated steam power plant has been done using a mathematical model. The working fluid in the power cycle is steam and the properties of the steam at different points in the cycle have been determined according to IAPWS standards using EES software. Development of an actual T-s diagram of the cycle and calculations of the mass balance for the simplified cycle has been conducted in EES [49]. Some parameters in the cycle are taken from the power plant archive and other parameters are determined using a T-s diagram, using EES software by finding out steam properties at different points and using the mass and energy balance of the necessary components. 1st law and 2nd law of thermodynamics have been applied to find out energy efficiency and exergy efficiency. The energy balance and exergy balance equation has been applied to find out the heat loss and destroyed exergy of the components [50,51]. After validating the code and methodology optimization potentiality is investigated which resulted in the integration of PTC with a stand-alone cycle. Several case studies have been analyzed by taking different configurations of feedwater heaters. The obtained results are compared with

Table 1
Power plant operating conditions. [48].

Operating conditions	value	unit
Total Power produced	200	MW
Power consumption	14	MW
Mass flow rate of fuel	54	Nm ³ /h
Heat rate	10448.6	kJ/kWh
Steam flow rate, mainline	670	Ton/h
Steam pressure, mainline	13	MPa
Steam temperature, mainline	540	°C
Water temperature, to boiler	247	°C
Boiler Pressure	15.9	MPa
Superheating temperature	850	K
Condenser Pressure	0.017	MPa
Combined Pump/motor efficiency	95	%

previous literature works. Most promising cases are further investigated, and a parametric study has been conducted to present a clear understanding of the effect of varying different operating parameters. The components considered for the analysis are as follows.

- Boiler
- High-Pressure Turbine (HPT)
- Low-Pressure Temperature (LPT)
- Low Pressure Closed Feed Water Heaters (LPH)
- High Pressure Closed Feed Water Heaters (HPH)
- Boiler feed pump
- Condenser
- Intermediate Pressure Turbine (IPT)
- Open Feed Water Heaters (Degaerator)

3.3. Governing equations

The general mass balance, energy balance, and exergy balance equations used for each component are stated below.

$$\text{MassBalanceEquation} : \sum \dot{m}_i = \sum \dot{m}_o \quad (1)$$

$$\text{EnergyBalanceEquation} : \dot{Q} - \dot{W} = \sum \dot{m}_o h_o - \sum \dot{m}_i h_i \quad (2)$$

$$\text{ExergyBalanceEquation} : \dot{W} + \sum \dot{m}_i \psi_i = \dot{Q} + \sum \dot{m}_o \psi_o \quad (3)$$

$$\text{TotalExergyofflow} : \dot{E}_x = \dot{m} \psi = \dot{m} [(h - h_0) - T_0(s - s_0)] \quad (4)$$

3.4. Mass balance equations

This mass balance is done based on the ideal T-s diagram, as shown in Fig. 3. The steam properties at different points on the T-s diagram are determined by EES software using ideal assumptions (for example-isentropic relations in pump and turbine and constant pressure relation in boiler, condenser, and feed water heaters). The T-s diagrams are given below. The Mass flow rate of extracted steam at different stages under ideal conditions is shown in Table 2.

$$HPH - 7x = \frac{h_1 - h_{45}}{h_{49} - h_{48}} \quad (5)$$

$$HPH - 6y = \frac{x(h_{44} - h_{47}) + (h_{45} - h_{42})}{(h_{46} - h_{44})} \quad (6)$$

$$HPH - 5z = \frac{(h_{42} - h_{38}) + (h_{40} - h_{43})(x + y)}{(h_{39} - h_{40})} \quad (7)$$

$$\text{Degaeratorm} = \frac{(x + y + z)(h_{34} - h_{41}) + (h_{37} - h_{34})}{(h_{36} - h_{34})} \quad (8)$$

$$LPH - 4n = \frac{(1 - x - y - z - m)(h_{34} - h_{30})}{(h_{35} - h_{33})} \quad (9)$$

$$LPH - 3o = \frac{(1 - x - y - z - m)(h_{30} - h_{27}) + n(h_{29} - h_{32})}{(h_{31} - h_{29})} \quad (10)$$

$$LPH - 2p = \frac{(n + o)(h_{25} - h_{28}) + (1 - x - y - z - m - n - o)(h_{23} - h_{22})}{(h_{24} - h_{22} - h_{25} - h_{23})} \quad (11)$$

$$LPH - 1q = \frac{(1 - x - y - z - m - n - o - p)(h_{22} - h_{17})}{(h_{19} - h_{20})} \quad (12)$$

3.5. Analysis of various key components of power cycle

The basis of thermodynamic analysis of different components and

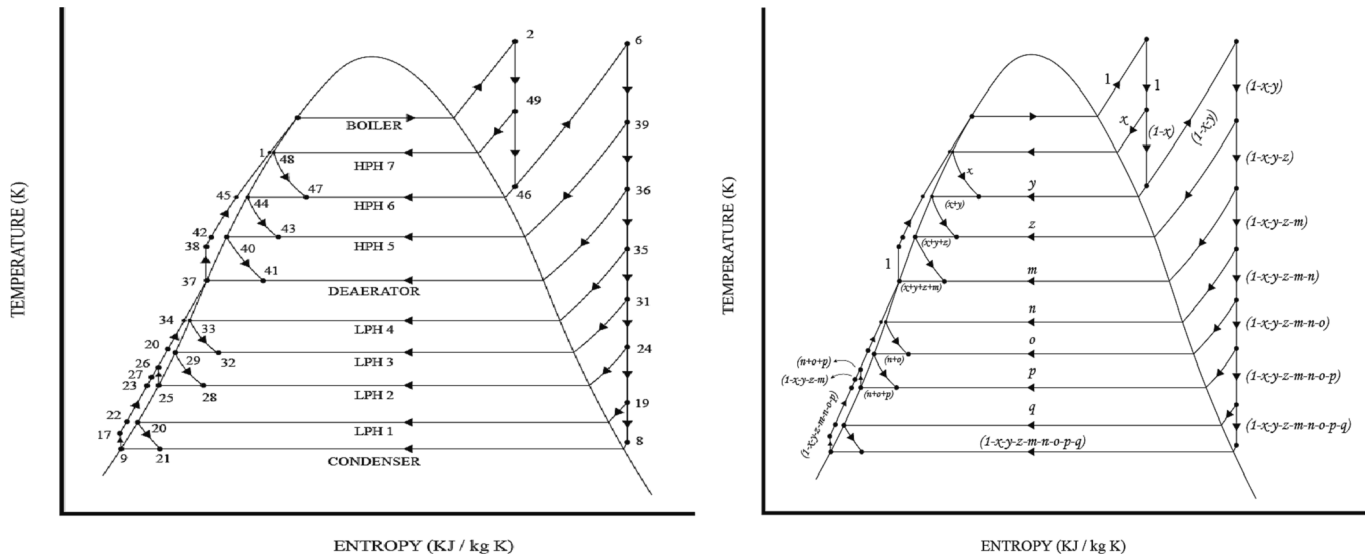


Fig. 3. Idealized t-s diagram showing the mass flow rate through different components.

Table 2
Mass flow rate of extracted steam at different stages under ideal conditions.

Components	Extracted steam	Mass Flowrate (kg/s)
HPH-7	x	0.05791
HPH-6	y	0.1055
HPH-5	z	0.009052
Deaerator	m	0.01022
LPH-4	n	0.04464
LPH-3	o	0.03158
LPH-2	p	0.05965
LPH-1	q	0.03296

corresponding governing equations are stated below.

High-Pressure Turbine (HPT): In this power plant, three stages of turbines are used- High-Pressure Turbine, Intermediate Pressure Turbine, and Low-Pressure Turbine. The High-Pressure Turbine has one extraction point.

Intermediate Pressure Turbine (IPT): The intermediate pressure turbine has 4 extraction points, and it is the maximum among 3-stages of turbines.

Low Pressure Turbine (LPT): The low-pressure turbine has one extraction point.

Closed Feed Water Heaters: Closed feed water heaters are counter-blow heat exchangers in which the extracted steam and feed water don't mix. In the simplified cycle, there are a total of 7 closed feed water heaters. 4 of them are Low-Pressure Heater (LPH) and 3 of them are High Pressure Heater (HPH).

Open Feed Water Heater (Deaerator): In open feed water heater the extracted steam mixes with the main feed water flow. The deaerator in this power cycle does the work of open feed water heater [52].

Condenser: Steam circulates from the low-pressure turbine to condenser through auxiliary components. For simplification, those have been merged. Lost heat from the cooling tower and condenser is considered the same in the calculation. It has been assumed that there is no leak from the glands of turbines and all the valves.

Boiler Feed Pump (BFP): The function of the boiler feed pump is to feed the water to the boiler and raise its pressure to the boiler operating pressure. Pumps are run by the electricity produced by the generator using the turbines. The energy loss of the BFP is taken from the base paper and the exergy loss is calculated using equation.

Boiler: The boiler is one of the main components which transfers heat to the feed water. The maximum portion of heat is transferred to the

working fluid through boiler. It is the component where the phase of the feed water is changed and is converted into steam. When fuel is burned its chemical energy is converted into thermal energy and this energy is transferred to the boiler. The fuel used in this power plant is natural gas. Chemical exergy has been considered when calculating the total power input in the boiler [53].

Governing Equations

$$\text{Energy Balance HPT } \dot{W}_{HPT} = \dot{m}_3 h_3 - \dot{m}_4 h_4 - \dot{m}_{49} h_{49} - \dot{Q}_{l,HPT} \quad (13)$$

$$\text{IPT } \dot{W}_{IPT} = \dot{m}_6 h_6 - \dot{m}_{50} h_{50} - \dot{m}_{35} h_{35} - \dot{m}_{31} h_{31} - \dot{m}_{24} h_{24} - \dot{m}_7 h_7 - \dot{Q}_{l,IPT} \quad (14)$$

$$\text{LPT } \dot{W}_{LPT} = \dot{m}_7 h_7 - \dot{m}_{19} h_{19} - \dot{m}_8 h_8 - \dot{Q}_{l,LPT} \quad (15)$$

$$\text{LPH } - 1 \dot{Q}_{l,LPH-1} = \dot{m}_{19} (h_{19} - h_{20}) - \dot{m}_{17} (h_{18} - h_{17}) \quad (16)$$

$$\text{LPH } - 2 \dot{Q}_{l,LPH-2} = \dot{m}_{24} h_{24} + \dot{m}_{22} h_{22} + \dot{m}_{28} h_{28} - \dot{m}_{25} h_{25} - \dot{m}_{23} h_{23} \quad (17)$$

$$\text{LPH } - 3 \dot{Q}_{l,LPH-3} = \dot{m}_{31} h_{31} + \dot{m}_{27} h_{27} + \dot{m}_{32} h_{32} - \dot{m}_{30} h_{30} - \dot{m}_{29} h_{29} \quad (18)$$

$$\text{LPH } - 4 \dot{Q}_{l,LPH-4} = \dot{m}_{35} h_{35} + \dot{m}_{30} h_{30} - \dot{m}_{33} h_{33} - \dot{m}_{34} h_{34} \quad (19)$$

$$\text{HPH } - 5 \dot{Q}_{l,HPH-5} = \dot{m}_{39} h_{39} + \dot{m}_{38} h_{38} + \dot{m}_{43} h_{43} - \dot{m}_{40} h_{40} - \dot{m}_{42} h_{42} \quad (20)$$

$$\text{HPH } - 6 \dot{Q}_{l,HPH-6} = \dot{m}_{46} h_{46} + \dot{m}_{42} h_{42} + \dot{m}_{47} h_{47} - \dot{m}_{45} h_{45} - \dot{m}_{44} h_{44} \quad (21)$$

$$\text{HPH } - 7 \dot{Q}_{l,HPH-7} = \dot{m}_{49} h_{49} + \dot{m}_{45} h_{45} - \dot{m}_1 h_1 - \dot{m}_{48} h_{48} \quad (22)$$

$$\text{Condenser } \dot{Q}_c = \dot{m}_8 (h_8 - h_9) + \dot{m}_{21} (h_{21} - h_9) - \dot{m}_{10} (h_{10} - h_{12}) \quad (23)$$

$$\text{Boiler } \dot{Q}_b = \dot{m}_5 (h_6 - h_5) + \dot{m}_1 (h_2 - h_1) \quad (24)$$

$$\text{Deaerator } \dot{Q}_{l,De} = \dot{m}_{36} h_{36} + \dot{m}_{41} h_{41} + \dot{m}_{34} h_{34} - \dot{m}_{37} h_{37} \quad (25)$$

$$\text{Exergy Balance HPT } \dot{W}_{HPT} = \dot{m}_3 \psi_3 - \dot{m}_4 \psi_4 - \dot{m}_{49} \psi_{49} - \dot{I}_{destroyed,HPT} \quad (26)$$

$$\text{IPT } \dot{W}_{IPT} = \dot{m}_6 \psi_6 - \dot{m}_{50} \psi_{50} - \dot{m}_{35} \psi_{35} - \dot{m}_{31} \psi_{31} - \dot{m}_{24} \psi_{24} - \dot{m}_7 \psi_7 - \dot{I}_{destroyed,IPT} \quad (27)$$

$$\text{LPT } \dot{W}_{LPT} = \dot{m}_7 \psi_7 - \dot{m}_{19} \psi_{19} - \dot{m}_{18} \psi_{18} - \dot{I}_{destroyed,LPT} \quad (28)$$

$$LPH - 1\dot{I}_{LPH-1} = T_0[\dot{m}_{19}(\psi_{19} - \psi_{20}) - \dot{m}_{17}(\psi_{18} - \psi_{17})] \quad (29)$$

$$LPH - 2\dot{I}_{LPH-2} = T_0[\dot{m}_{24}\psi_{24} + \dot{m}_{22}\psi_{22} + \dot{m}_{28}\psi_{28} - \dot{m}_{25}\psi_{25} - \dot{m}_{23}\psi_{23}] \quad (30)$$

$$LPH - 3\dot{I}_{LPH-3} = T_0[\dot{m}_{31}\psi_{31} + \dot{m}_{27}\psi_{27} + \dot{m}_{32}\psi_{32} - \dot{m}_{30}\psi_{30} - \dot{m}_{29}\psi_{29}] \quad (31)$$

$$LPH - 4\dot{I}_{LPH-4} = T_0[\dot{m}_{35}\psi_{35} + \dot{m}_{30}\psi_{30} + \dot{m}_{33}\psi_{33} - \dot{m}_{34}\psi_{34}] \quad (32)$$

$$HPH - 5\dot{I}_{HPH-5} = T_0[\dot{m}_{39}\psi_{39} + \dot{m}_{38}\psi_{38} + \dot{m}_{43}\psi_{43} - \dot{m}_{40}\psi_{40} - \dot{m}_{42}\psi_{42}] \quad (33)$$

$$HPH - 6\dot{I}_{HPH-6} = T_0[\dot{m}_{46}\psi_{46} + \dot{m}_{42}\psi_{42} + \dot{m}_{47}\psi_{47} - \dot{m}_{45}\psi_{45} - \dot{m}_{44}\psi_{44}] \quad (34)$$

$$HPH - 7\dot{I}_{HPH-7} = T_0[\dot{m}_{49}\psi_{49} + \dot{m}_{45}\psi_{45} - \dot{m}_1\psi_1 - \dot{m}_{48}\psi_{48}] \quad (35)$$

$$\text{Condenser } \dot{I}_c = \dot{m}_8\psi_8 + \dot{m}_{21}\psi_{21} + \dot{m}_{12}\psi_{12} - \dot{m}_{10}\psi_{10} - \dot{m}_9\psi_9 \quad (36)$$

$$\text{Boiler } \dot{I}_b = \dot{X}_{ch} + \dot{m}_5\psi_5 + \dot{m}_1\psi_1 - \dot{m}_6\psi_6 - \dot{m}_2\psi_2 \quad (37)$$

$$BFP\dot{I}_{BFP} = \dot{m}_{37}h_{37} - \dot{m}_{38}h_{38} - 0.3968 \quad (38)$$

$$\text{Deaerator } \dot{I}_{De} = T_0[\dot{m}_{36}\psi_{36} + \dot{m}_{41}\psi_{41} + \dot{m}_{34}\psi_{34} - \dot{m}_{37}\psi_{37}] \quad (39)$$

$$\text{1st Law Efficiency } HPT\eta_{1,HPT} = \frac{\dot{W}_{HPT}}{\dot{m}_3h_3 - \dot{m}_4h_4 - \dot{m}_{49}h_{49}} \quad (40)$$

$$IPT\eta_{1,IPT} = \frac{\dot{W}_{IPT}}{\dot{m}_6h_6 - \dot{m}_{50}h_{50} - \dot{m}_{35}h_{35} - \dot{m}_{31}h_{31} - \dot{m}_{24}h_{24} - \dot{m}_7h_7} \quad (41)$$

$$LPT\eta_{1,LPT} = \frac{\dot{W}_{LPT}}{\dot{m}_7h_7 - \dot{m}_{19}h_{19} - \dot{m}_8h_8} \quad (42)$$

$$LPH - 1\eta_{1,LPH-1} = \frac{\dot{m}_{17}(h_{18} - h_{17})}{\dot{m}_{19}(h_{19} - h_{20})} \quad (43)$$

$$LPH - 2\eta_{1,LPH-2} = \frac{\dot{m}_{25}h_{25} + \dot{m}_{23}h_{23}}{\dot{m}_{24}h_{24} + \dot{m}_{22}h_{22} + \dot{m}_{28}h_{28}} \quad (44)$$

$$LPH - 3\eta_{1,LPH-3} = \frac{\dot{m}_{30}h_{30} + \dot{m}_{29}h_{29}}{\dot{m}_{31}h_{31} + \dot{m}_{27}h_{27} + \dot{m}_{32}h_{32}} \quad (45)$$

$$LPH - 4\eta_{1,LPH-4} = \frac{\dot{m}_{30}(h_{30} - h_{34})}{\dot{m}_{35}(h_{35} - h_{33})} \quad (46)$$

$$HPH - 5\eta_{1,HPH-5} = \frac{\dot{m}_{40}h_{40} + \dot{m}_2h_{42}}{\dot{m}_{39}h_{39} + \dot{m}_{38}h_{38} + \dot{m}_{43}h_{43}} \quad (47)$$

$$HPH - 6\eta_{1,HPH-6} = \frac{\dot{m}_{45}h_{45} + \dot{m}_{44}h_{44}}{\dot{m}_{46}h_{46} + \dot{m}_{42}h_{42} + \dot{m}_{47}h_{47}} \quad (48)$$

$$HPH - 7\eta_{1,HPH-7} = \frac{\dot{m}_{45}(h_{45} - h_1)}{\dot{m}_{49}(h_{49} - h_{48})} \quad (49)$$

$$\text{Deaerator } \eta_{1,De} = \frac{\dot{m}_{37}h_{37}}{\dot{m}_{36}h_{36} + \dot{m}_{41}h_{41} + \dot{m}_{34}h_{34}} \quad (50)$$

$$\eta_{2,HPT} = \frac{\dot{W}_{HPT}}{\dot{m}_3\psi_3 - \dot{m}_4\psi_4 - \dot{m}_{49}\psi_{49}} \quad (51)$$

$$IPT\eta_{2,IPT} = \frac{\dot{W}_{IPT}}{\dot{m}_6\psi_6 - \dot{m}_{50}\psi_{50} - \dot{m}_{35}\psi_{35} - \dot{m}_{31}\psi_{31} - \dot{m}_{24}\psi_{24} - \dot{m}_7\psi_7} \quad (52)$$

$$LPT\eta_{2,LPT} = \frac{\dot{W}_{LPT}}{\dot{m}_7\psi_7 - \dot{m}_8\psi_8 - \dot{m}_{19}\psi_9} \quad (53)$$

$$LPH - 1\eta_{2,LPH-1} = \frac{\dot{m}_{17}(\psi_{18} - \psi_{17})}{\dot{m}_{19}(\psi_{19} - \psi_{20})} \quad (54)$$

$$LPH - 2\eta_{2,LPH-2} = \frac{\dot{m}_{25}\psi_{25} + \dot{m}_{23}\psi_{23}}{\dot{m}_{24}\psi_{24} + \dot{m}_{22}\psi_{22} + \dot{m}_{28}\psi_{28}} \quad (55)$$

$$LPH - 3\eta_{2,LPH-3} = \frac{\dot{m}_{30}\psi_{30} + \dot{m}_{29}\psi_{29}}{\dot{m}_{31}\psi_{31} + \dot{m}_{27}\psi_{27} + \dot{m}_{32}\psi_{32}} \quad (56)$$

$$LPH - 4\eta_{2,LPH-4} = \frac{\dot{m}_{30}(\psi_{30} - \psi_{34})}{\dot{m}_{35}(\psi_{35} - \psi_{33})} \quad (57)$$

$$HPH - 5\eta_{2,HPH-5} = \frac{\dot{m}_{40}\psi_{40} + \dot{m}_{42}\psi_{42}}{\dot{m}_{39}\psi_{39} + \dot{m}_{38}\psi_{38} + \dot{m}_{43}\psi_{43}} \quad (58)$$

$$HPH - 6n_{2,HPH-6} = \frac{\dot{m}_{45}\psi_{45} + \dot{m}_{44}\psi_{44}}{\dot{m}_{46}\psi_{46} + \dot{m}_{42}\psi_{42} + \dot{m}_{47}\psi_{47}} \quad (59)$$

$$HPH - 7\eta_{2,LPH-7} = \frac{\dot{m}_{45}(\psi_{45} - \psi_1)}{\dot{m}_{49}(\psi_{49} - \psi_{48})} \quad (60)$$

$$\text{Deaerator } \eta_{2,De} = \frac{\dot{m}_{37}\psi_{37}}{\dot{m}_{36}\psi_{36} + \dot{m}_{41}\psi_{41} + \dot{m}_{34}\psi_{34}} \quad (61)$$

3.6. Area analysis of PTC and fuel consumption calculations

Collector area has been determined from the amount of heat that has to be added to the feed water by the solar farm. Fuel consumption has been calculated for the base cycle and repowered cycle. From that fuel saving has been analyzed. Calculation is done according to the equations and specifications in reference to [29,39].

$$\text{Collector Area : } A_c = \frac{Q_f}{DNI \times \eta_c} m^2 \quad (62)$$

$$\text{Specific fuel consumption : } b = \frac{122.8}{\eta_1} = \frac{122.8 \times Q_b}{3600 \times N_e} \text{ g/kWh} \quad (63)$$

$$\text{Heat input in the boiler for repowered cycle : } Q_b^R = \frac{3600 \times N_e^R}{\eta_1^R} - Q_f \text{ kJ/h} \quad (64)$$

$$\text{Fuel consumption : } B_f = 122.8 \times Q_b \quad (65)$$

$$B_f^R = 122.8 \times Q_b^R \text{ Kg/h} \quad (66)$$

$$\text{Fuel Saving Due to repowering } \Delta B_f = B_f - B_f^R \text{ Kg/h} \quad (66)$$

3.7. Mathematical framework

The framework of the study and workflow is depicted in Fig. 4. Analytical work is done in EES software with IAPWS standard steam properties. Input parameters are defined, and components are coded sequentially. Pressure and temperature drops follow the power plant database from Ahmadi et al.'s study [48]. EES generates a parametric table, cross-validated with actual power plant data [48]. Some differences exist due to simplifications during modeling. Performance of key components are compared, confirming simulation validity. For model validation, optimization involves case studies, simulating zero mass flow rate across replaced FWHs. This affects major components, revealing increased output and efficiency but with a condenser performance decrease as the temperature at the condenser outlet increases with increase in flow rate. Practical cases are selected for parametric analysis based on condenser sizing criteria, exploring cycle sensitivity to varying parameters. The most optimal case is analyzed for exergy loss across major components, identifying improvement opportunities.

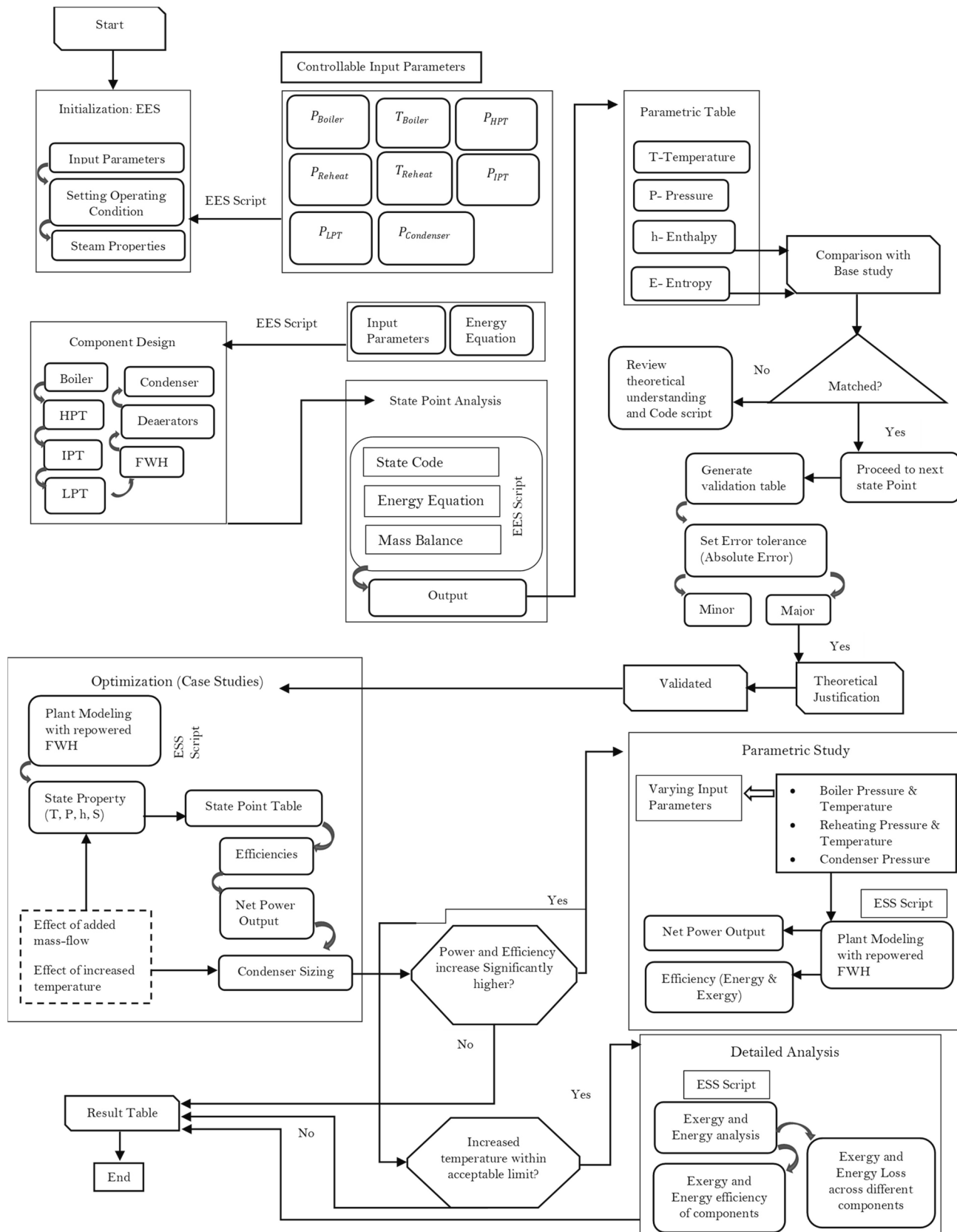


Fig. 4. Mathematical modeling framework and workflow diagram.

4. Model validation

Table 3 shows the comparison between simulation results with existing power plant's node properties obtained from archive data [48]. **Table 4** presents performance comparison of key components based on simulation and study conducted on the existing power plant by Ahmadi et al. The results are in good agreement with the archive data except for some points. For those nodes theoretical analysis using mass and energy balance have been conducted and obtained values were justified which indicates the authenticity of model validation. However, for some points minor irregularities are observed due to the implication of different libraries for property determination.

5. Analysis of power plant for various scenarios

Various extraction points closure scenarios have been studied to analyze their impact on unit power output and overall efficiency. **Table 5**, **Table 6**, and **Table 7** depict cases with single, double, and triple extractions, respectively. Each case includes information on the cut-off node, affected turbine, and operation conditions, illustrations of the repowered heater and corresponding T-S diagram. The solar farm section involves feed water heating by PTC. Single extractions (Cases 1–6)

affect specific turbines, showcasing varied outcomes. Double extractions (Cases 7–12) impact individual or paired turbines, resulting in diverse mass flow rate increases and unit load output gains. Triple extractions (Cases 13 and 14) affect multiple turbines, notably boosting unit load output. However, some cases pose challenges for stable plant operation and condenser performance despite increased output and efficiency. Parametric study has been conducted on promising cases to understand the impact of different parameters on unit load output and overall energy and exergy efficiency.

6. Result and discussion

6.1. Overview

Through tables and graphics, the results section provides insights for 14 case studies, parametric and energy-exergy analyses. For every scenario, **Table 9** presents detailed information on increased mass flow rates, turbine outputs, cut-off nodes, discarded FWHs, unit load output, and overall cycle efficiencies. **Figs. 6 and 7** show how energy and energy efficiency vary between scenarios, whereas **Fig. 5** compares the load outputs for each case with the original power plant.

The subsequent sections focus on a parametric study of the four most

Table 3
Comparison of obtained node properties from simulation and power plant archive database.

Node	Properties from Power Plant Archive			Present Simulation			Error T	h	s
	T(K)	h(kJ/kg)	s(kJ/kg.K)	T(K)	h(kJ/kg)	s(kJ/kg.K)			
1	519	1066	2.726	519	1067	2.726	0	1	2.725
2	813.1	3444	6.576	813.1	3445	6.576	0	1	6.574
3	813.1	3477	6.733	813.1	3478	6.733	0	1	6.731
4	606.2	3079	6.716	605.9	3080	6.716	0.3	1	6.714
5	606.2	3079	6.716	605.9	3080	6.716	0.3	1	6.714
6	813.1	3552	7.458	813.1	3553	7.458	0	1	7.452
7	450	2828	7.624	450	2828	7.624	0	0	7.622
8	318.2	188.4	0.6393	318.2	188.7	0.6393	0	0.3	0.6385
9	308.2	146.7	0.5058	308.2	146.9	0.5058	0	0.2	0.5049
10	318.2	188.5	0.6392	318.2	188.7	0.6392	0	0.2	0.6385
11	318.2	188.6	0.6392	318.2	188.8	0.6392	0	0.2	0.6386
16	312.2	163.6	0.5596	312.2	163.8	0.5596	0	0.2	0.5588
17	312.3	165.9	0.559	312.2	165.3	0.559	0.1	0.6	0.5608
18	322.5	207.9	0.6906	322.2	207	0.6906	0.3	0.9	0.6939
19	344.1	297.2	0.9667	344.1	297.1	0.9667	0	0.1	0.9671
20	329.1	234.4	0.7882	329.7	236.9	0.7882	0.6	2.5	0.7807
21	329.1	234.4	0.7882	329.7	236.9	0.7882	0.6	2.5	0.7807
22	325.1	219.1	0.7295	325.2	219.3	0.7295	0.1	0.2	0.7288
23	357.7	354.9	1.122	357.2	353.1	1.122	0.5	1.8	1.128
24	443.2	2814	7.581	443	2814	7.581	0.2	0	7.58
25	378.5	441.5	1.362	378	439.6	1.362	0.5	1.9	1.366
26	379.3	445.8	1.372	379	444.8	1.372	0.3	1	1.374
27	360.1	365.2	1.158	360.2	365.7	1.158	0.1	0.5	1.156
28	386.3	2697	1.443	386.3	470.6	1.443	0	2226.4	7.298
29	385.3	470.3	1.442	385.3	470.6	1.442	0	0.3	1.442
30	384.5	467.6	1.431	384.3	467	1.431	0.2	0.6	1.432
31	532.3	2987	7.612	532.3	2988	7.612	0	1	7.61
32	430.5	2779	1.924	430.2	662.7	1.924	0.3	2116.3	7.177
33	430.5	664.4	1.913	430.2	662.7	1.913	0.3	1.7	1.917
34	432.1	671.5	1.929	431.8	669.8	1.929	0.3	1.7	1.933
35	644.2	3209	7.617	644.2	3210	7.617	0	1	7.617
36	720.3	3361	7.505	720	3361	7.505	0.3	0	7.504
37	438.3	698.3	1.993	441.4	711.5	1.993	3.1	13.2	1.995
38	440	715.5	1.993	440	713.7	1.993	0	1.8	1.989
39	721.2	3365	7.505	720	3361	7.505	1.2	4	7.557
40	459	2784	6.508	459	2785	6.508	0	1	6.551
41	459	2809	2.196	459	789	2.196	0	2020	6.78
42	454.5	777.8	2.13	454.5	777.8	2.13	0	0	2.13
43	511.6	2911	6.605	511.6	2831	6.605	0	80	6.813
44	511.6	2830	6.268	511.6	2831	6.268	0	1	6.265
45	489.3	930.7	2.457	489.5	931.9	2.457	0.2	1.2	2.455
46	603.6	3073	6.707	603.6	3074	6.707	0	1	6.703
47	507.6	2817	6.238	507	2816	6.238	0.6	1	6.24
48	507.6	1011	2.643	507	1009	2.643	0.6	2	2.649
49	679.2	3268	6.834	697	3268	6.834	0.2	0	6.832
50	720.3	3361	7.505	720	3361	7.505	0.3	0	7.504

Table 4

Comparison of key components' performances from simulation with the existing power plant.

Component	Energy efficiency Existing Plant	Simulation	Deviation(abs)	Exergy efficiency Existing plant	simulation	Deviation(abs)
Boiler	90.55 %	90.22 %	0.33	44.5 %	45.2 %	0.7
HPT	87.67 %	89.76 %	2.09	78.28 %	80.93 %	2.65
IPT	91.08 %	92.78 %	1.7	87.34 %	86.75 %	0.59
LPT	82.62 %	82.95 %	0.33	80.62 %	81.80 %	1.18
Cycle	32 %	33.69 %	1.69	35.2 %	36.53 %	1.33

feasible cases. The effects of changing input parameters on net unit load output and energy-exergy efficiency are shown in Fig. 9 through Fig. 13. Case 12 stands as the most promising taking condenser sizing into consideration. The in-depth examination in the following section, which is illustrated by Figs. 14 and 15, presents energy and exergy efficiency for both the total cycle and major components. Fig. 16 (a) and (b) graphically depict the loss percentages and magnitudes for each component, emphasizing the large losses in the condenser and boiler. Details on losses in various FWs are shown in Table 10. Table 8 presents the properties of all nodes on the power plant. The table has been generated from EES code. Flow exergy $\psi(\text{kJ/kg})$ has been obtained with respect to reference surrounding temperature and pressure.

6.2. Case studies

Increase in mass flow ranges from a minimum of 4.72 kg/s in Case 6 to a maximum of 25.10 kg/s in Case 13. While this added mass flow significantly boosts power, it also poses a critical consideration for condenser sizing. Addressing this impact is vital in the design of a feed water repowering system. This added mass flow decreases the generating load to preserve the vacuum in the condenser as referred to in different studies [29].

In the condenser, just enough vacuum must be maintained so that the steam flow from the turbines can fully enter into the condenser uninterrupted otherwise backflow of steam could happen from the condenser towards the turbine which greatly reduces the total power output from the turbines. The condenser vacuum level is relevant because it can affect the condensation temperature of the steam when the flow rate of hot steam is increased. If the flow rate of hot steam is increased while maintaining the same vacuum level and cooling water conditions, it is likely to lead to a higher condensation temperature.

Among all the cases, case 12 was selected for a more detailed study even though it exhibited lower power output and efficiencies compared to cases 7, 13 & 14 which are impractical considering condenser sizing to maintain that necessary vacuum pressure. Case 12 stands out because the increase in condenser temperature in this scenario remains within an acceptable limit, making it a suitable and practical choice. The total work output is another very crucial parameter to judge the performance of any power plant, which signifies the comprehensive power production of the system, exhibiting significant variation among various designs. Such as Case 13 exhibited the maximum aggregated work production of 261.30 MW, while Case 6 exhibited the minimum output of 186.62 MW. Nevertheless, Case 12 represents a balance between work output and condenser temperature increase. There is considerable variation in the efficiency of energy and exergy, with Case 13 being identified as the configuration that exhibits the maximum level of efficiency. This particular configuration demonstrates superior performance in terms of overall work production and energy efficiency followed by cases 14, 7 & 12.

Fig. 5 illustrates the comparisons between the power output of the original cycle and various configurations of the modified cycle. In each of the cases, there has been a noticeable rise in the net power output as compared to the initial power output as the conventional feed water heaters have been substituted by PTC feed water heaters. There are notable increases in net power production in cases 1, 7, 12, 13, and 14.

Highest power output is in case 13 which is due to the greatest mass flow increase in the cycle for closing triple extractions.

Fig. 6 and Fig. 7 show the energy efficiency and exergy efficiency enhancement in modified scenarios over base cycle respectively. Both efficiencies increase corresponding to net power output increase. Case 13 has the highest energy and exergy efficiency about 43.6 % and 48.1 % respectively owing to the largest power output. Efficiency increment over unmodified base cycle is 10.7 % and 11.6 % for energy and exergy respectively.

The graph depicted in Fig. 8 (a) illustrates the different solar collector areas needed for various configurations (cases) of the repowered cycle. The main factors that impact the necessary area of solar collectors are the total heat input required for the feed water heater by the solar farm, the average direct normal sunlight irradiance (DNI) at the power plant's location, and the efficiency of the solar collectors. The Direct Normal Irradiance (DNI) value used for this calculation in Isfahan is 800 W/m^2 [29]. The collector efficiency has been assumed to be 60 % [29]. According to the Figure, the case with the highest demand for solar collector area is case 13, which is approximately $1.74 \times 10^5 \text{m}^2$. This is followed by case 14 and case 12, which require areas of $1.41 \times 10^5 \text{m}^2$ and $1.16 \times 10^5 \text{m}^2$ respectively. The situation that necessitates the greatest amount of heat input to the feed water heater by the solar farm will result in the highest value for the needed solar collector area, assuming that the DNI value and collector efficiency remain constant throughout all cases. Fig. 8 (b) illustrates the fuel savings resulting from cycle repowering using solar energy in various scenarios. The fuel savings are quantified in kilograms per hour. Case 13 exhibits the most significant fuel-saving rate, amounting to 1691.46 kg/hour.

6.3. Parametric analysis (Cases 1,2,7 and 14)

Parametric analysis is performed to understand the effect of changing different operating parameters on the system performance. The study has been conducted by varying boiler temperature and pressure, reheating temperature and pressure, and condenser pressure. The findings have been illustrated below and discussed.

6.3.1. Effect of variation of main steam temperature

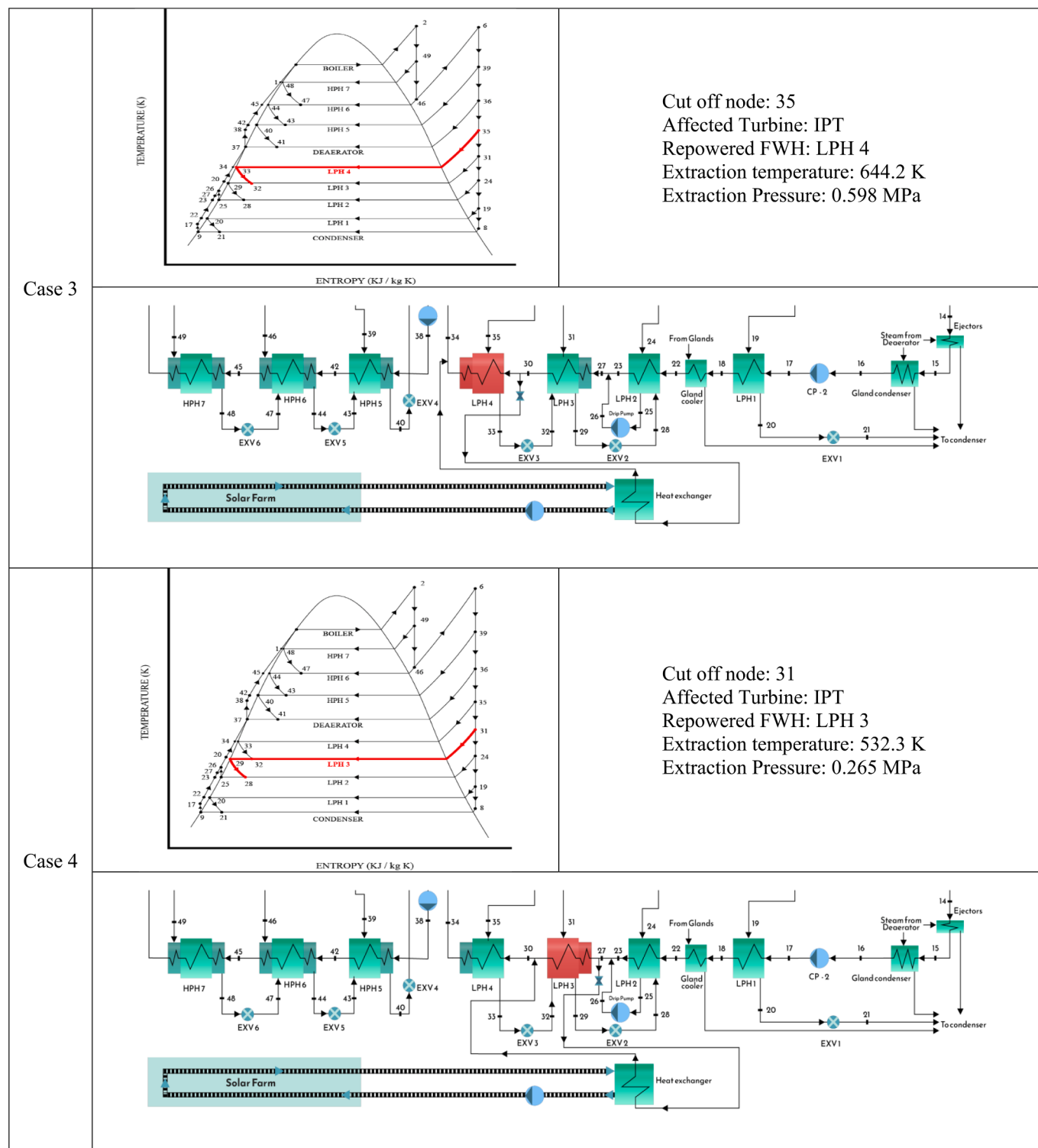
Main steam temperature variation effect on output and efficiencies of the cycle has been illustrated in Fig. 9. Fig. 9 (a) shows a positive correlation between steam temperature and power output as the main temperature increases within the range of 798 K to 823 K, the net output also increases, and it exhibits a linear trend. However, the slope is steeper for case 2 compared to other cases. Case 7 results in the highest net power output of 235.38 MW corresponding to the highest steam temperature.

A similar trend is noticeable in total energy and exergy efficiency of the cycle from Fig. 9 (b). A higher power output is evidence of a more efficient cycle for the same heat input. Case 7 and Case 12 show a close similarity in terms of their overall efficiency but there is substantial difference in increase mass flow rate which is 17.94 kg/s and 11.37 kg/s, respectively. The disparity between these two mass flow rates has a significant impact on condenser sizing. In case 7, the condenser temperature exhibited an approximate increase of 6 K in comparison to case 12. Based on cycle efficiency and the feasibility of operating conditions,

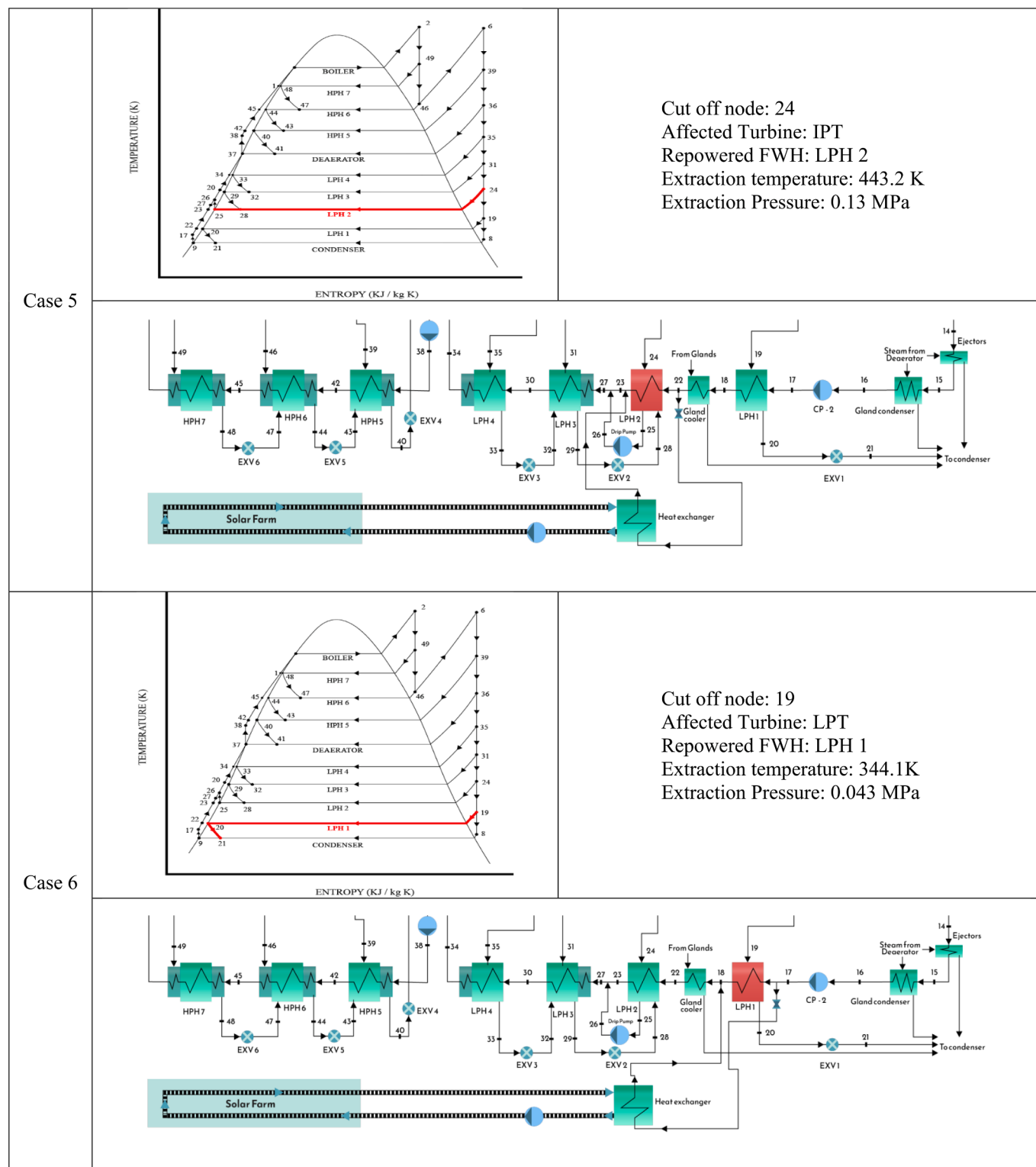
Table 5
Cases considered for cutting off a single extraction.

ID	T-s diagram	Reflections
Case 1		<p>Cut off node: 49 Affected Turbine: HPT Repowered FWH: HPH 7 Extraction temperature: 679.2 K Extraction Pressure: 4.151 MPa</p>
Case 2		<p>Cut off node: 46 Affected Turbine: HPT Repowered FWH: HPH 6 Extraction temperature: 603.6 K Extraction Pressure: 2.802 MPa</p>

(continued on next page)

Table 5 (continued)

(continued on next page)

Table 5 (continued)

case 12 poses greater prospects.

6.3.2. Effect of variation of main steam pressure

The effect of varying main steam pressure on the net power output and cycle efficiency have been illustrated in Fig. 10 (a) and Fig. 10(b). Fig. 10(a) depicts the net power output of the cycle, where the pressure

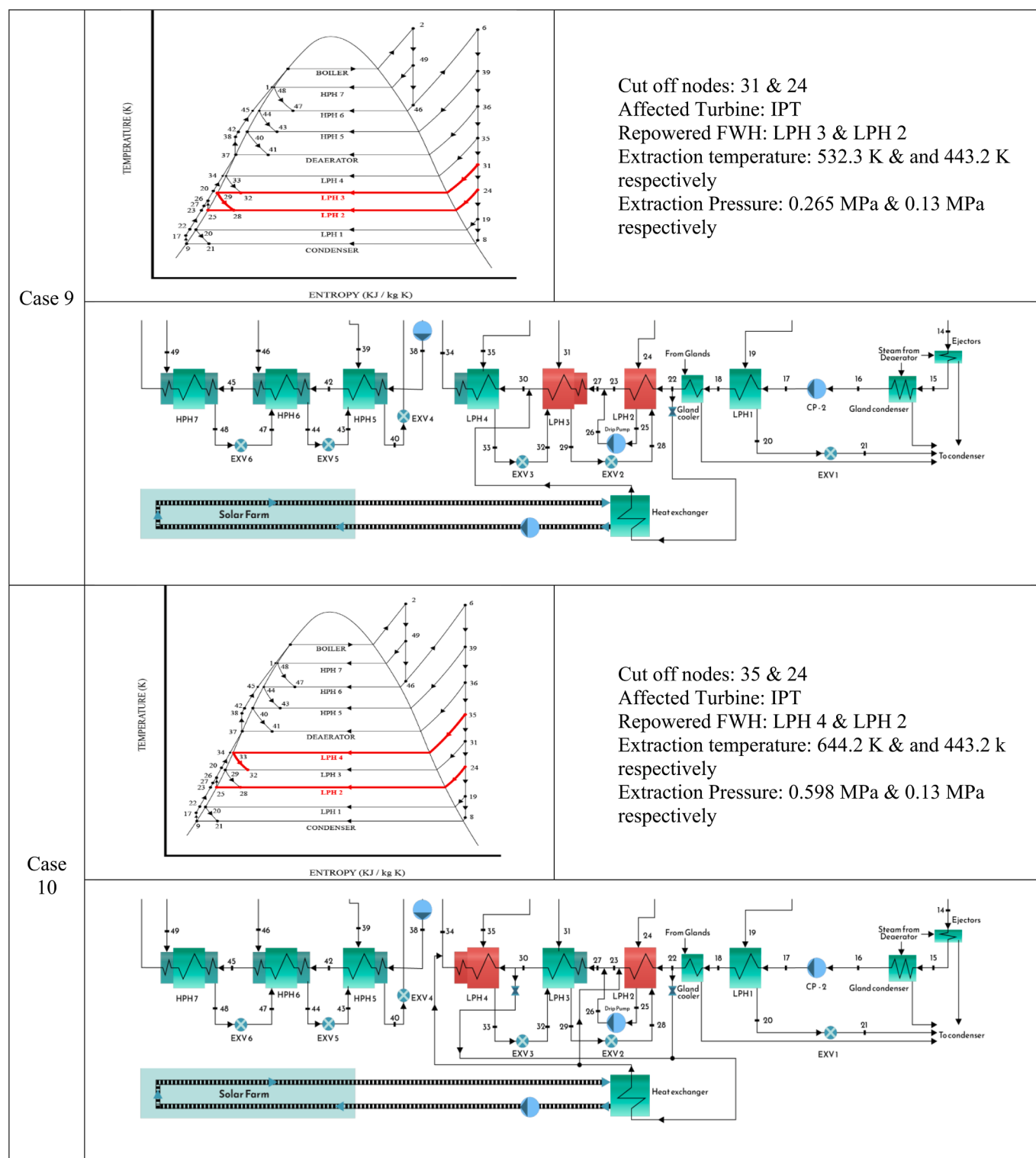
is varied within the range of 12 to 14 MPa. It is evident that, in all the cases, the output has a positive correlation with the increase in pressure, reaching its peak at 12.5 MPa. The output is steady within the range of 12.5 to 13 MPa. This observation signifies the stable operational state of the current cycle. The net power output experiences a large increase when the pressure is further elevated from 13 to 14 MPa. Case 7 stands

Table 6

Cases considered for cutting off a double extraction.

ID	TS diagram	Reflections
		Cut off nodes: 49 & 46 Affected Turbine: HPT Repowered FWH: HPH 7 & HPH 6 Extraction temperature: 679.2 K & 603.6 K respectively Extraction Pressure: 4.151 MPa & 2.802 MPa respectively
Case 7		
Case 8		Cut off nodes: 35 & 31 Affected Turbine: IPT Repowered FWH: LPH 4 & LPH 3 Extraction temperature: 644.2 K & 532.3 K respectively Extraction Pressure: 0.598 MPa & 0.265 MPa respectively

(continued on next page)

Table 6 (continued)

(continued on next page)

Table 6 (continued)

Case 11		Cut off nodes: 24 & 19 Affected Turbine: IPT and LPT Repowered FWH: LPH 2 & LPH 1 Extraction temperature: 443.2 K & and 344.1 k respectively Extraction Pressure: 0.13 MPa & 0.043 MPa respectively
Case 12		Cut off nodes: 49 & 35 Affected Turbine: HPT and IPT Repowered FWH: HPH 7 & LPH 4 Extraction temperature: 679.2 K & and 644.2 K respectively Extraction Pressure: 4.151 MPa & 0.598 MPa respectively

as the most substantial enhancement, followed by cases 12, 1, and 2, at a pressure of 14 MPa. The power output is approximately 243.10 MW. At a constant pressure between 12.5 and 13 MPa, the power output reaches approximately 230 MW. The efficiencies exhibit an identical trend as shown in Fig. 10(b). The rise in net power output is positively correlated with the increase in efficiencies. The maximum energy efficiency and exergy efficiency are approximately 41 % and 45 % respectively. Both case 7 and case 12 have identical characteristics.

6.3.3. Effect of variation of reheat steam temperature

Fig. 11 (a) and Fig. 11(b) demonstrate that an increase in reheat steam temperature leads to an increase in net power output and overall efficiency for each case. In each case, there is a consistent linear efficiency increase within the range of reheating temperatures from 798 K to 823 K. The highest output for case 7 is 234.85 MW at a reheating temperature of 823 K. The energy and exergy efficiencies are obtained to be around 40.73 % and 45.03 %, respectively.

Table 7

Cases considered for cutting off a triple extraction.

ID	T-s diagram	Reflections
Case 13		Cut off nodes: 49, 46 & 35 Affected Turbine: HPT and IPT Repowered FWH: HPH 7, HPH 6 & LPH 4 Extraction temperature: 679.2 K, 603.6 K & 644.2 K respectively Extraction Pressure: 4.151 MPa, 2.802 MPa & 0.598 MPa respectively
Case 14		Cut off nodes 49, 46 & 31 Affected Turbine: HPT and IPT Repowered FWH: HPH 7, HPH 6 & LPH 3 Extraction temperature: 679.2 K, 603.6 K & 532.3 K respectively Extraction Pressure: 4.151 MPa, 2.802 MPa & 0.265 MPa respectively

6.3.4. Effect of variation of reheat steam pressure

Fig. 12 (a) and Fig. 12(b) illustrate the effect of varying the reheat steam pressure within the range of 2.2 to 2.5 MPa on the net power output and overall cycle efficiency, respectively. It illustrates a linear relationship between the power output and the reheating pressure, in contrast to the fluctuation in boiler pressure. From the study, case 7 exhibits the most substantial rise, followed by case 12, case 1, and case

2. The cycle's output at case 7, with a reheating pressure of 2.5 MPa, has been measured to be 232.52 MW. The corresponding energy and exergy efficiencies are determined to be 40.49 % and 44.78 %, respectively.

6.3.5. Effect of variation of condenser pressure

The power output and overall efficiency of the cycle are significantly influenced by the operating pressure and temperature of the condenser.

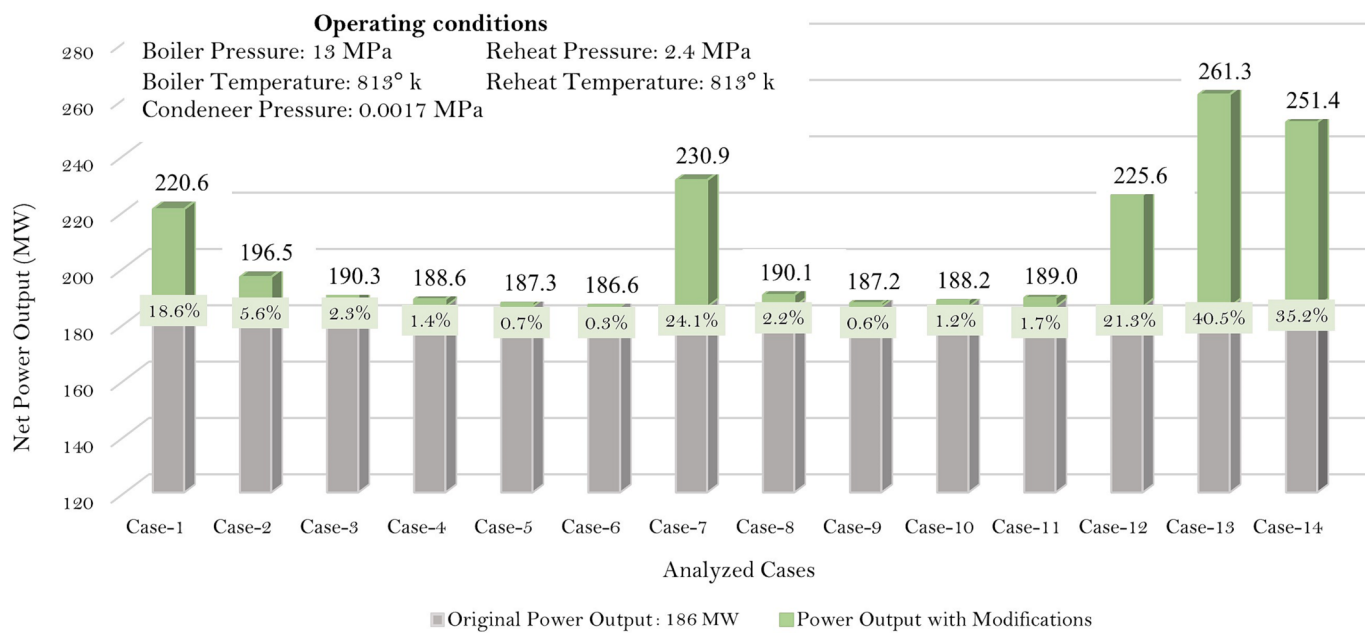


Fig. 5. Output comparison (percentage increase) of different cases with the original power plant maintaining similar operating conditions.

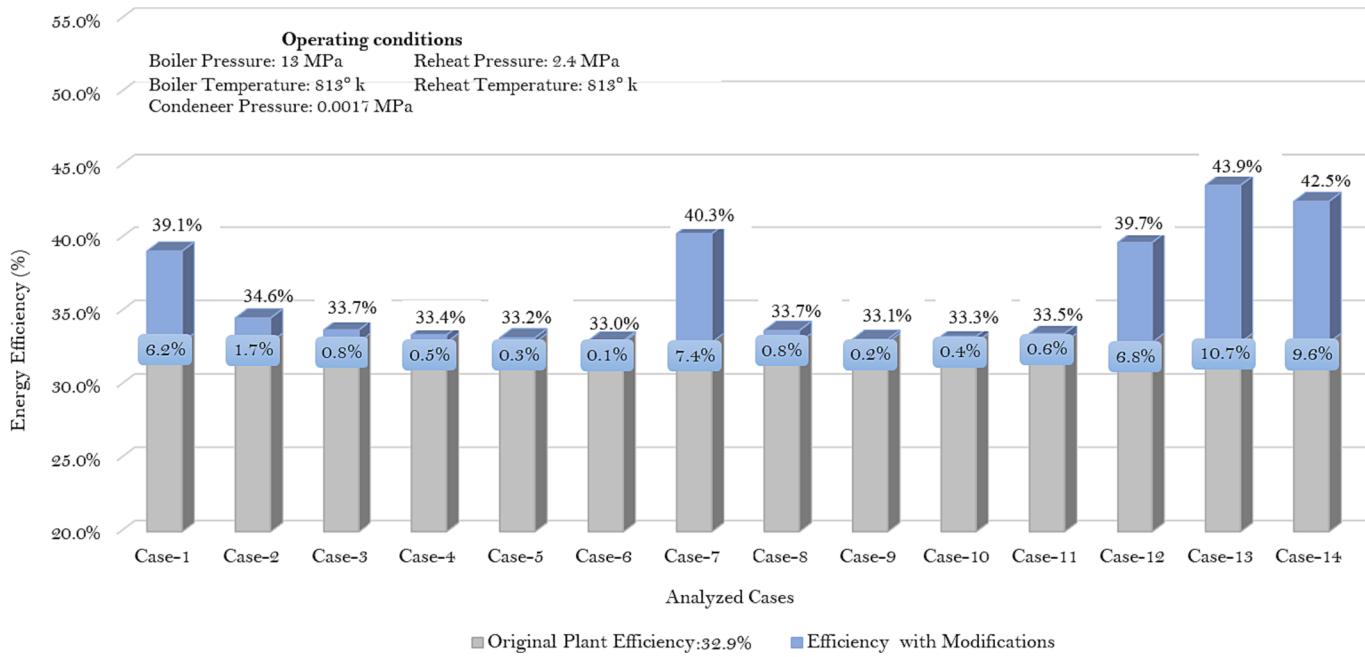


Fig. 6. Energy efficiency in different cases.

When both pressure and temperature increase, it indicates a greater amount of usable energy being dissipated or released into the environment. The impact of raising the condenser pressure on production and efficiency is seen in Fig. 13 (a) and Fig. 13(b). It shows a decline in both power output and overall efficiency, namely in terms of energy and exergy which aligns with the principles of thermodynamics. In each investigated scenario about a range of condenser pressure, both energy and exergy efficiencies exhibit a decline of 2 %. Additionally, the power output experiences a reduction of around 10 MW.

6.4. Detailed analysis: Case-12

Earlier it has been mentioned that case-12 has been considered to be

the most suitable scenario even though it generates less power at a lower efficiency in comparison with case-13,14 and 7. Cases 13 and 14 have been identified as unfeasible cases as the increased mass flow rate indicates impractical condenser sizing. However, between case-12 and case-7, case-12 produces lower power output but with almost the same efficiency as case-7, handling significantly less added mass flowrate of 11.37 kg/s which is about 17.94 kg/s in case-7. That's why case-12 has been considered for the detailed analysis. The following section provides findings of detailed energy and exergy analysis of case-12.

6.4.1. Cycle and component efficiencies (Case-12)

Fig. 14 depicts the overall performance and presents the energy and exergy efficiency of the overall cycle for case 12 which are obtained to

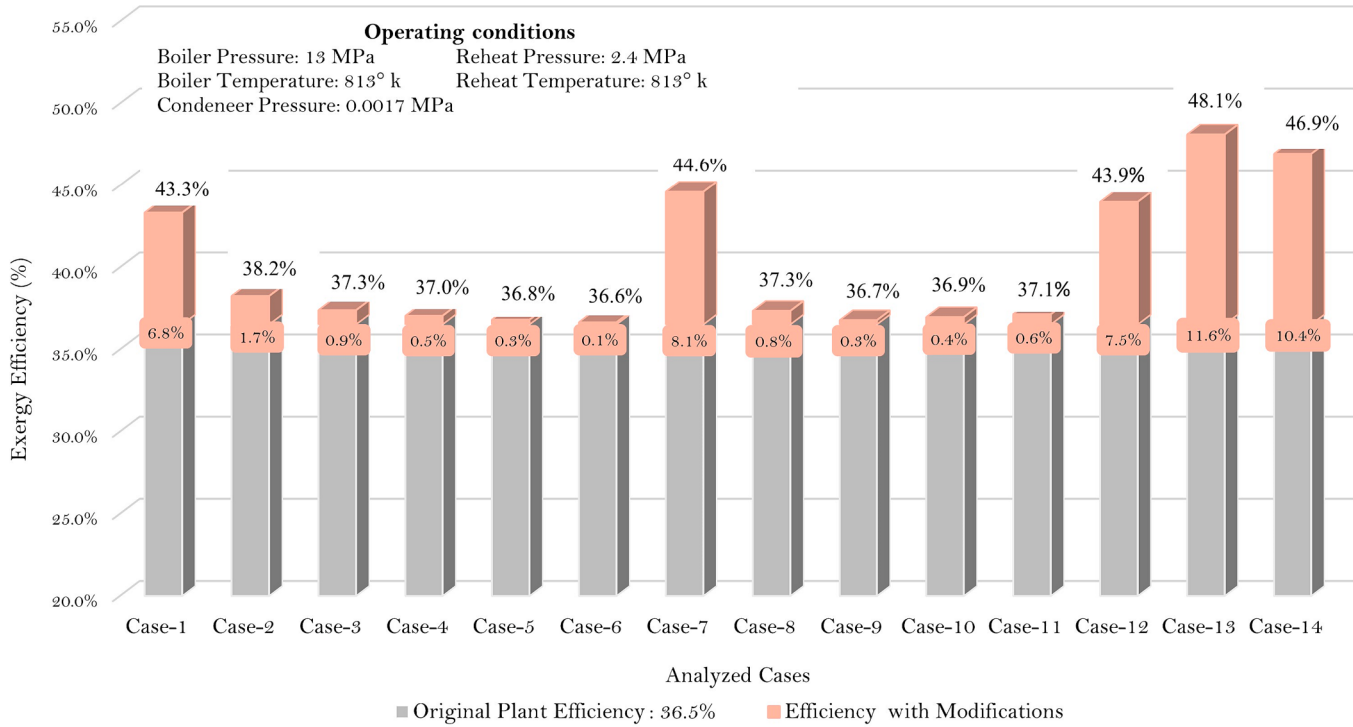


Fig. 7. Exergy efficiency in different cases.

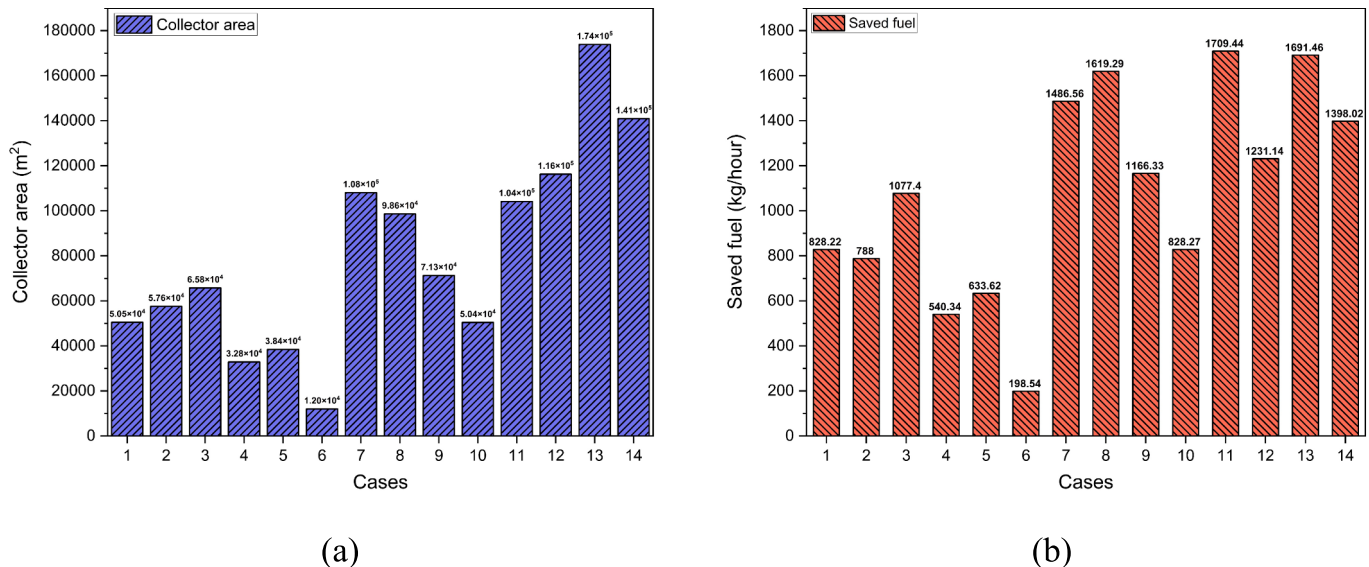


Fig. 8. A) solar collector area requirement b) fuel saving in different cases.

be 39.73 % and 43.99 % respectively. It produces around 225 MW of electricity while consuming around 14 MW for the operation of internal components. Lower efficiency indicates high fuel consumption at the boiler and high energy waste as the condenser.

Energy and exergy efficiencies have been computed for each component, as depicted in Fig. 15. The boiler exhibits the lowest exergy efficiency. The percentage is approximately 43.72 %. The observation pertains to the significant exergy loss occurring within the boiler. When considering turbines, it can be observed that the intermediate-pressure turbine has superior efficiency in both the first and second stages when compared to the high- and low-pressure turbines. The components exhibit energy and exergy efficiencies of around 92.78 % and 86.75 %, respectively, which are the highest values observed.

6.4.2. Energy and exergy losses in major components

The analysis of energy and exergy losses across major components reveals crucial insights for enhancing system efficiency. The holistic evaluation presented in Fig. 16 forms the basis for targeted optimization efforts, aiming to minimize energy wastage and maximize exergy efficiency, ultimately improving the overall system performance.

The condenser emerges as the primary contributor to energy losses, accounting for a substantial 289.65 MW (75.09 %) and an exergy loss of 239.42 MW (65.39 %). This underscores its pivotal role in system efficiency. Inadequate insulation of steam pipelines and suboptimal maintenance contribute to increased energy and exergy losses. Proper insulation and maintenance practices are crucial for minimizing these losses. The boiler, while significant, contributes 51.35 MW (13.31 %) in

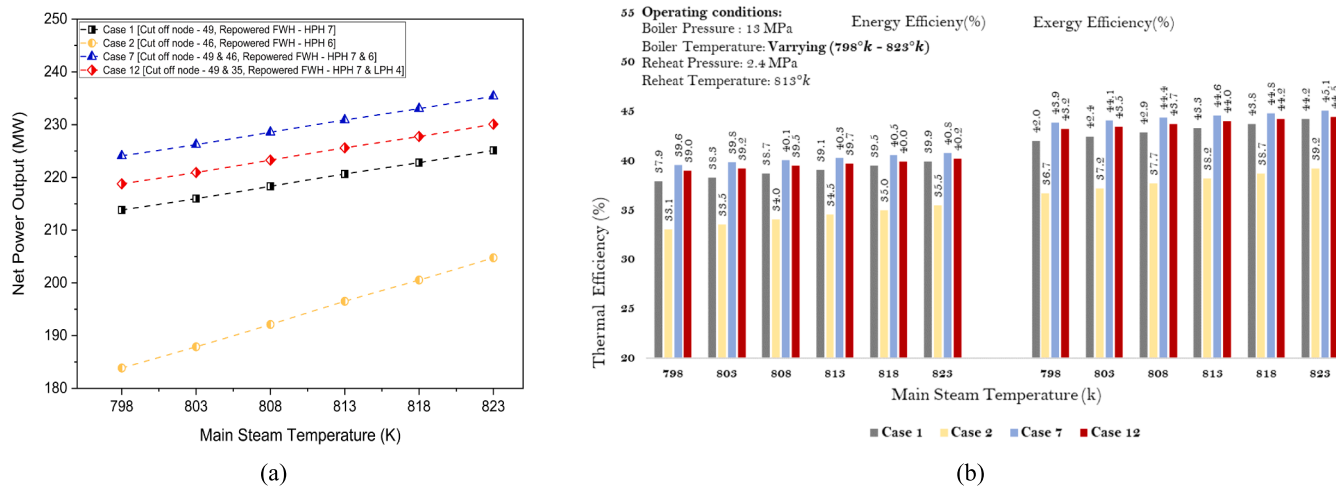


Fig. 9. Effect of variation of main steam temperature on (a) Net Power Output (b) Thermal Efficiency of feasible cases.

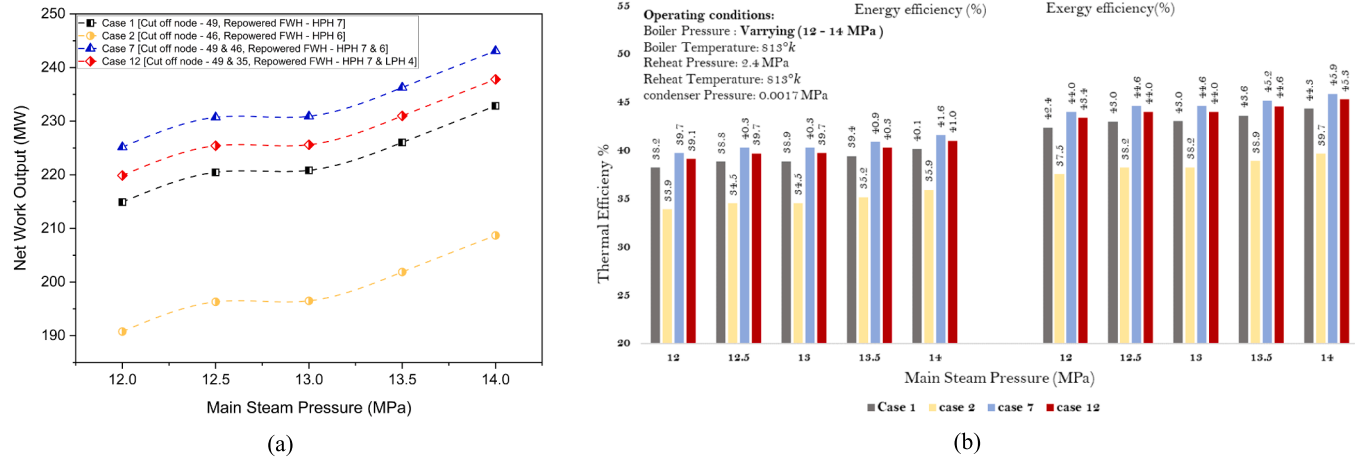


Fig. 10. Effect of variation of main steam pressure on (a) Net Power Output (b) Thermal Efficiency of feasible cases.

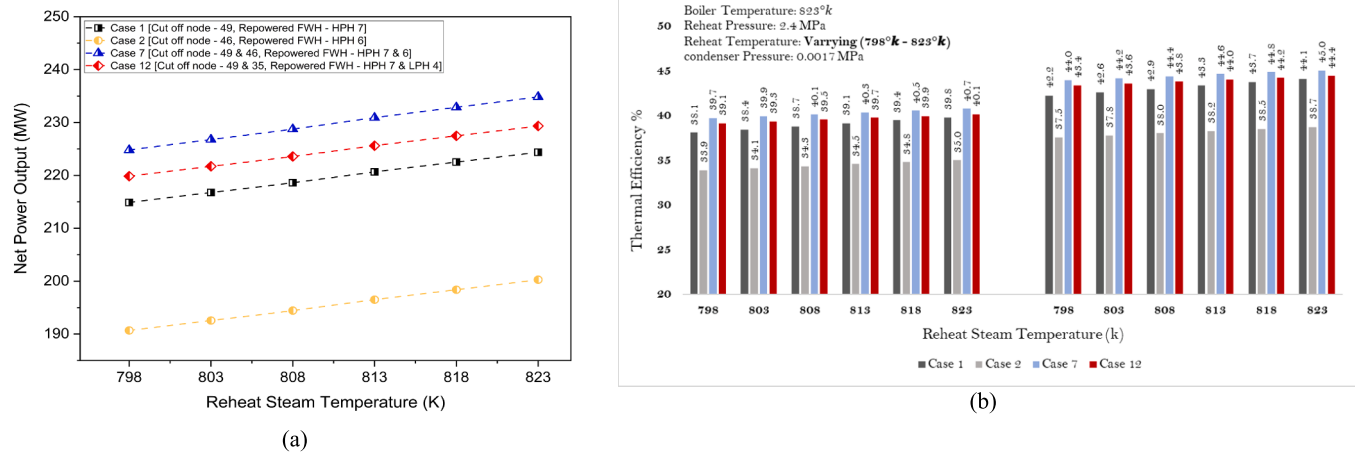
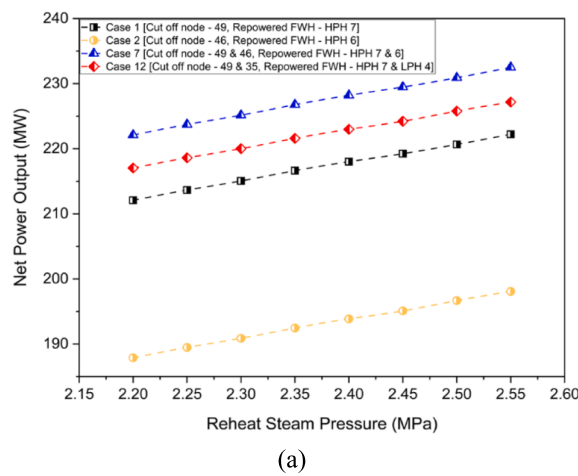


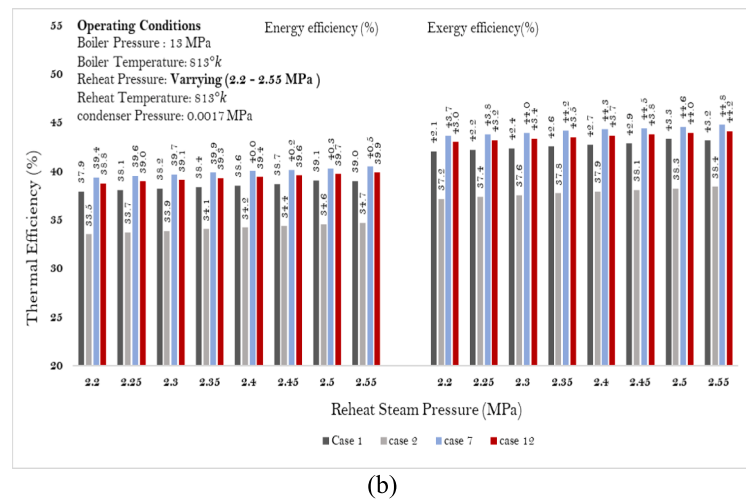
Fig. 11. Effect of varying reheat steam temperature on a) Net Power Output b) Thermal Efficiency of feasible cases.

energy loss but the largest exergy loss of 317.53 MW (86.55 %). This results from incomplete combustion of fuel and losses due to thermal radiation at high temperatures. Mitigating these losses requires optimizing fuel quality and combustion processes. Utilizing materials with

reduced emissivity and improved insulation can effectively mitigate thermal radiation losses, enhancing exergy efficiency. Therefore, addressing losses in both the boiler and condenser is paramount for substantial overall performance improvement.

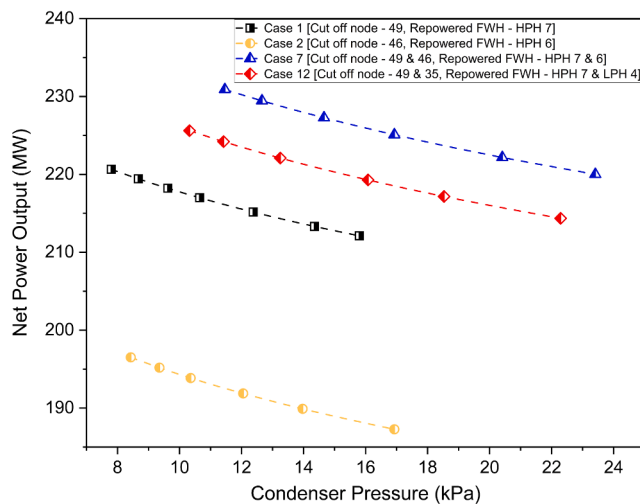


(a)



(b)

Fig. 12. Effect of varying reheat steam pressure on a) Net Power Output b) Thermal Efficiency on feasible cases.



(a)

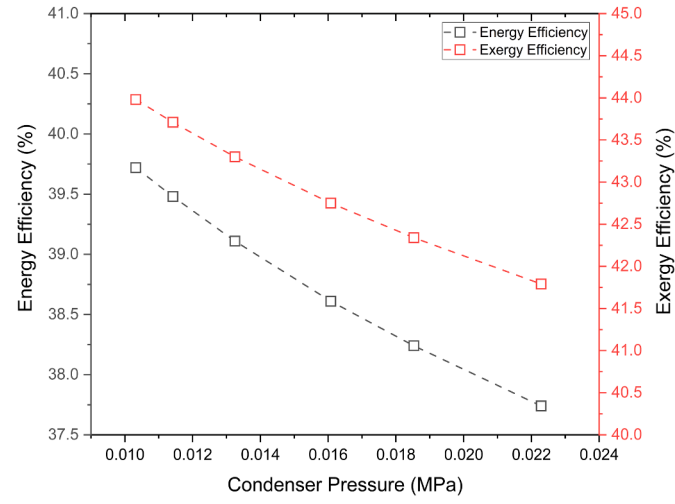


Fig. 13. Effect of condenser pressure on (a) net power output (b) cycle efficiencies of the feasible cases.

The High-Pressure Turbine (HPT) exhibits a notable yet manageable energy loss of 12.45 MW (3.23 %) and an exergy loss of 8.69 MW (2.37 %). Similarly, the Intermediate-Pressure Turbine (IPT) experiences an energy loss of 17.83 MW (4.62 %) and an exergy loss of 16.52 MW (4.51 %). The Low-Pressure Turbine (LPT) contributes 11.75 MW (3.05 %) in energy loss and 12.38 MW (3.37 %) in exergy loss. These results are due to aerodynamic losses, mechanical friction, and thermal losses. These inefficiencies can result from suboptimal blade designs, steam quality variations, and internal friction within the turbine components. Additionally, incomplete expansion of steam and unavoidable heat dissipation contribute to energy losses. To mitigate these losses, optimizing turbine blade designs, fine-tuning operational parameters, and employing materials that minimize frictional losses are crucial strategies. While these losses are relatively modest, optimizing these components can contribute to system-wide efficiency improvements. The Boiler Feed Pump (BFP) and Condensate Water Pump (CWP), with minor roles, exhibit energy losses of 1.76 MW (0.46 %) and 0.93 MW (0.24 %), respectively. For exergy losses, BFP contributes 0.81 MW (0.22 %), and CWP contributes 1.39 MW (0.38 %). Though minor, these components should not be overlooked in comprehensive system optimization efforts.

Feed water heaters are very crucial elements for the power plants. A portion of the steam flow which can produce some extra work output if

it's let to pass through the turbine, is extricated from the turbine and used to heat the feed water. So, any form of inefficiencies i.e.; energy or exergy loss across these heaters have a significant impact on the cycle. As in case 12, HPH 7 and LPH 4 have been repowered by solar energy, exergy and energy analysis have been performed for the remaining feed water heaters to obtain the effectiveness of heating process and losses associated within these are presented in Table 10.

Among all the heaters, LPH 2 exhibits the most energy loss of 7.03 MW and HPH 5 has the greatest exergy loss of 1.44 MW. The efficiency can be enhanced by the utilization of more compact and sophisticated heat exchangers, as well as by maximizing the heat transfer area. The efficiency of the cycle is influenced by the quantity of heat exchangers employed. The overall efficiency demonstrates an upward trend when the number of heaters is increased, reaching its peak between 4 and 6 units. The incremental gain in efficiency using more heaters than these are insufficient to justify the additional expenses and complications associated with the cycle.

7. Conclusion

Integration of renewable energy sources with conventional power plants holds immense prospects. This study represents repowering po-

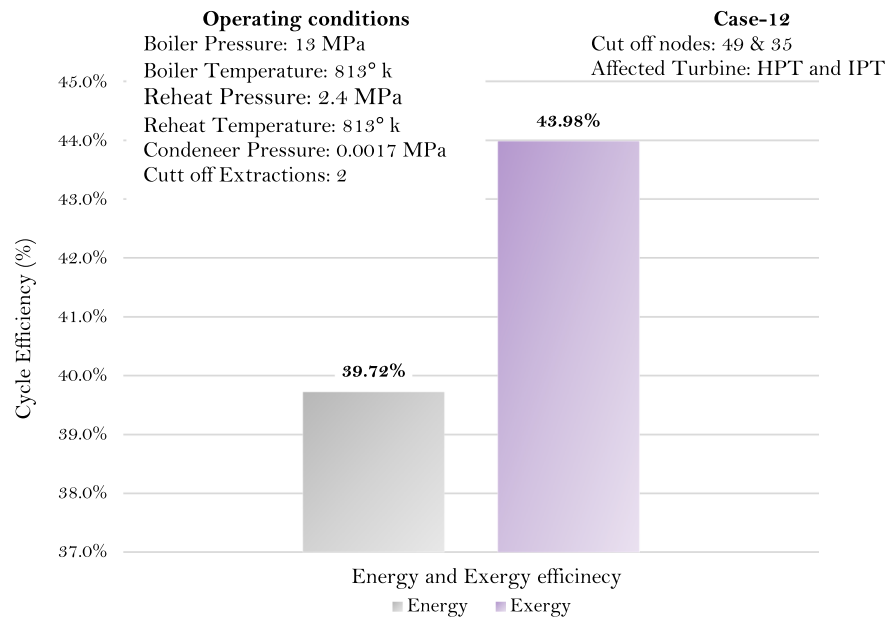


Fig. 14. Energy and exergy efficiency of overall cycle for case-12.

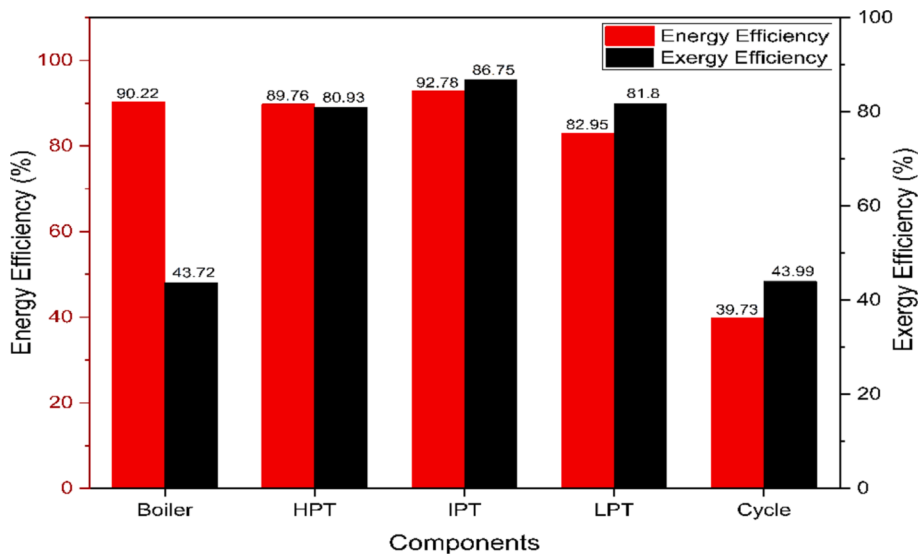


Fig. 15. Energy & Exergy efficiency of major components in case-12.

tentiality of 200 MW Shahid Montazeri Power plant in Iran with CSP. Effects of replacing traditional FWHs with PTC solar farm to preheat the feed water has been investigated thoroughly. Demonstrating the significant implications of this solar-thermal hybrid power generation strategies, performance of the selected power plant has been assessed for 14 different cases. Key Findings of this study are:

- o Retrofitting power plants with solar energy is a very promising aspect for better plant performance.
- o Replacing FWHs with PTC solar farm results in increased efficiency and power output than original cycle in all 14 cases. Maximum energy efficiency of 43.69 % and output of 261 MW has been obtained in case 13.
- o Replacing HPHs and a greater number of heaters have higher effect on the performance of power plant.
- o The design with triple extractions has shown the most impressive improvement in power output and cycle efficiency

- o Highest solar collector area of 173842.18 m^2 is required for necessary feed water heating in case 13.
- o Solar repowering substantially reduces the fuel consumption and environmental impact.
- o Condenser sizing has a major impact on the power plant performance.
- o Case 12 is the most feasible approach and it is sensitive to different operating parameters.
- o Major exergy and energy losses are associated with boiler and condenser respectively.

This study has highlighted possible optimization configurations and scope of improvements in a power plant for boosting the performance and ensuring sustainable electricity generation.

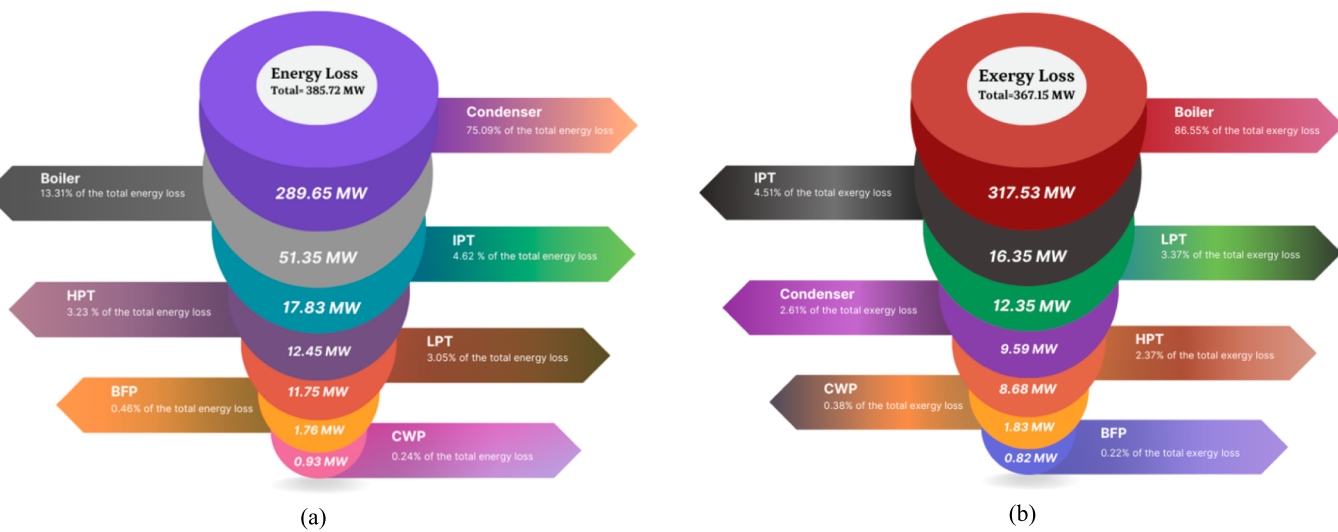


Fig. 16. Losses across major components (a) Energy (b) Exergy and percentages.

Table 8
Simulated node property of existing power plant.

Node	T(K)	P(MPa)	m (kg/s)	h(kJ/kg)	s (kJ/kg K)	ψ (kJ/kg)	Ex (MW)
1	519	17	179.4	1067	2.726	259.2476	46.50902
2	813.1	13	179.4	3445	6.576	1489.948	267.2966
3	813.1	9.9	179.4	3478	6.733	1476.162	264.8234
4	605.9	2.8	171.4	3080	6.716	1083.228	184.6255
5	605.9	2.8	161.5	3080	6.716	1083.228	173.9616
6	813.1	2.4	161.5	3553	7.458	1335.112	215.6205
7	450	0.127	137.841	2828	7.624	560.6436	77.27967
8	318.2	0.017	133.121	188.7	0.6393	2.7842	0.370635
9	308.2	0.075	137.841	146.9	0.5058	0.7672	0.105752
10	318.2	0.075	6944	188.7	0.6392	2.814	19.54042
11	318.2	0.215	6944	188.8	0.6392	2.914	20.23482
16	312.2	0.31	137.841	163.8	0.5596	1.6348	0.225342
17	312.2	1.95	137.841	165.3	0.559	3.3136	0.45675
18	322.2	1.75	137.841	207	0.6906	5.7968	0.799037
19	344.1	0.043	4.72	297.1	0.9667	13.619	0.064282
20	329.7	0.017	4.72	236.9	0.7882	6.612	0.031209
21	329.7	0.017	4.72	236.9	0.7882	6.612	0.031209
22	325.2	1.65	137.841	219.3	0.7295	6.5046	0.896601
23	357.2	1.45	137.841	353.1	1.122	23.3396	3.217154
24	443	0.13	5.5	2814	7.581	559.4576	3.077017
25	378	0.13	17.789	439.6	1.362	38.3196	0.681667
26	379	1.45	17.789	444.8	1.372	40.5396	0.721159
27	360.2	1.4	155.63	365.7	1.158	25.2116	3.923681
28	386.3	0.13	12.289	470.6	1.443	45.1816	0.555237
29	385.3	0.265	12.289	470.6	1.442	45.4796	0.558899
30	384.3	1.2	155.63	467	1.431	45.1576	7.027877
31	532.3	0.265	5.12	2988	7.612	724.2196	3.708004
32	430.2	0.265	7.169	662.7	1.924	93.9436	0.673482
33	430.2	0.6	7.169	662.7	1.913	97.2216	0.696982
34	431.8	0.9	155.63	669.8	1.929	99.5536	15.49353
35	644.2	0.6	7.169	3210	7.617	944.7296	6.772767
36	720	1.249	1.8	3361	7.505	1129.106	2.03239
37	441.4	0.77	179.4	711.5	1.993	122.1816	21.91938
38	440	15.5	179.4	713.7	1.993	124.3816	22.31406
39	720	1.249	4.07	3361	7.505	1129.106	4.59546
40	459	1.249	21.97	2785	6.508	850.2116	18.67915
41	459	0.75	21.97	789	2.196	139.1876	3.057952
42	454.5	18	179.4	777.8	2.13	147.6556	26.48941
43	511.6	1.249	17.9	2831	6.605	867.3056	15.52477
44	511.6	2.8	17.9	2831	6.268	967.7316	17.3224
45	489.5	17.5	179.4	931.9	2.457	204.3096	36.65314
46	603.6	2.8	9.9	3074	6.707	1079.91	10.69111
47	507	2.8	8	2816	6.238	961.6716	7.693373
48	507	4.15	8	1009	2.643	225.9816	1.807853
49	697	4.15	8	3268	6.834	1236.064	9.888509
50	720	1.249	5.87	3361	7.505	1129.106	6.62785

Table 9

Efficiency and power output for considered cases.

Case	Cut off extraction nodes	Repowered feed water heaters	Added mass (kg/s)	Increased workout across turbines (MW)			Increase of condenser temperature (K)	Total work output (MW) (With the effect of condenser temperature variation)	Heat Input from PTC SolarFarm to Feed Water (MW)	Energy efficiency (%)	Exergy efficiency (%)
				HPT	IPT	LPT					
1	49	HPH-7	8	25.96	5.8	2.4	6	220.65	24.23	39.11	43.33
2	46	HPH-6	9.94	0	7.21	3.05	7.45	196.51	27.64	34.55	38.25
3	35	LPH-4	7.16	0	3.1	2.9	5.37	190.36	31.56	33.74	37.39
4	31	LPH-3	5.12	0	1.2	2.2	3.84	188.65	15.76	33.44	37.05
5	24	LPH-2	5.5	0	0.01	2.3	4.12	187.39	18.44	33.22	36.81
6	19	LPH-1	4.72	0	0	1.2	3.54	186.62	5.74	33.08	36.65
7	49,46	HPH-7&6	17.94	26.14	13	5.49	13.45	230.90	51.88	40.33	44.61
8	35, 31	LPH-4&3	12.28	0	4	4	9.21	190.15	47.32	33.71	37.35
9	31, 24	LPH-3&2	10.62	0	1.2	3.2	7.96	187.27	34.20	33.19	36.78
10	24, 19	LPH-2&1	10.22	0	0.01	5.2	7.66	188.25	24.19	33.37	36.97
11	35, 24	LPH-4&2	12.66	0	3	4.1	9.49	189.09	50.00	33.52	37.14
12	49,35	HPH 7 & LHP 4	11.37	26.14	8.56	4.64	8.52	225.61	31.56	39.73	43.99
13	49, 46,35	HPH-7&6, LPH-4	25.1	26.14	41.21	7.69	19	261.30	83.44	43.69	48.11
14	49, 46,31	HPH-7&6, LPH-3	23.06	26.14	32.01	7.06	17.5	251.48	67.64	42.56	46.93

Table 10

Energy and exergy loss in heaters for case-12.

Components	Energy loss (MW)	Exergy loss (MW)
LPH 1	6.10	0.35
LPH 2	7.03	0.37
LPH 3	3.03	0.42
HPH 5	3.17	1.44
HPH 6	2.41	1.11

Future recommendations

This study focused on achieving optimal efficiency in thermal power plants. The findings provided significant insights that can contribute to future research endeavors in the development of key components. Moreover, the investigation revealed the innovative nature of the integration of renewable energy sources with conventional thermal power plants. This has the potential to be highly significant in the future. The design of PTC falls outside the purview of this study. However, the parametric framework presented in this research can be expanded upon to explore more effective methods for energy generation. Furthermore, it is feasible to carry out a study on multi-objective optimization, whereby an appropriate optimization technique can be employed to improve thermodynamic performance and assure efficient energy generation. This type of study would prove highly beneficial in establishing the foundational framework for subsequent investigations of a similar nature.

CRediT authorship contribution statement

Sifat Abdul Bari: Conceptualization, Data curation, Formal analysis, Investigation, Methodology, Software, Validation, Visualization, Writing – original draft. **Mohtasim Fuad:** Conceptualization, Data curation, Formal analysis, Investigation, Methodology, Software, Validation, Visualization, Writing – original draft. **Kazi Fahad Labib:** Formal analysis, Investigation, Visualization, Writing – original draft. **M. Monjurul Ehsan:** . Yasin Khan: Conceptualization, Supervision, Validation, Writing – review & editing, Project administration. **Muhammad Mahmood Hasan:** Project administration, Writing – review & editing, Conceptualization, Supervision.

Declaration of competing interest

The authors declare that they have no known competing financial interests or personal relationships that could have appeared to influence the work reported in this paper.

Data availability

Data will be made available on request.

References

- [1] “Fossil Fuels Made Up 82% of Global Energy Consumption in 2022: New Data.” <https://www.commondreams.org/news/fossil-fuels-global-energy-consumption> (accessed Jan. 20, 2024).
- [2] O. Gershon, J. K. Asafo, A. Nyarko-Asomani, and E. F. Koranteng, “Investigating the nexus of energy consumption, economic growth and carbon emissions in selected african countries,” Energy Strateg. Rev., vol. 51, no. October 2023, p. 101269, 2024, doi: 10.1016/j.esr.2023.101269.
- [3] S. Kılıç Depren, M. T. Kartal, N. Coban Çelikdemir, and Ö. Depren, “Energy consumption and environmental degradation nexus: A systematic review and meta-analysis of fossil fuel and renewable energy consumption,” Ecol. Inform., vol. 70, 2022, doi: 10.1016/j.ecoinf.2022.101747.
- [4] Ge Y, et al. Power/thermal-to-hydrogen energy storage applied to natural-gas distributed energy system in different climate regions of China. Energy Convers Manag 2023;283. <https://doi.org/10.1016/j.enconman.2023.116924>.
- [5] Kilkış Ş, Krajačić G, Duić N, Rosen MA, Al-Nimir MA. Sustainable development of energy, water and environment systems in the critical decade for climate action. Energy Convers Manag Nov. 2023;296:117644. <https://doi.org/10.1016/j.enconman.2023.117644>.
- [6] “Renewables,2023: Analysis and forecast to 2028.” International Energy Agency, 2023. [Online]. Available: <https://www.iea.org/reports/renewables-2023>.
- [7] Porto-Hernandez LA, et al. Fundamental optimization of steam Rankine cycle power plants. Energy Convers Manag 2023;289. <https://doi.org/10.1016/j.enconman.2023.117148>.
- [8] Reshael M, Javed A, Jamil A, Ali M, Mahmood M, Waqas A. Multiparametric optimization of a reheated organic rankine cycle for waste heat recovery based repowering of a degraded combined cycle gas turbine power plant. Energy Convers Manag 2022;254. <https://doi.org/10.1016/j.enconman.2022.115237>.
- [9] T. Srinivas, A. V. S. S. K. S. Gupta, and B. V. Reddy, “Generalized thermodynamic analysis of steam power cycles with ‘n’ number of feedwater heaters,” Int. J. Thermodyn., vol. 10, no. 4, 2007.
- [10] Y. A. Cengel, “Thermodynamics : An Engineering Approach INTRODUCTION AND BASIC CONCEPTS,” vol. 8th Editio, pp. 1–59, 2015.
- [11] A. Bejan, Advanced Engineering Thermodynamics. 2016. doi: 10.1002/9781119245964.
- [12] Wang Y, Cao L, Hu P, Li B, Li Y. Model establishment and performance evaluation of a modified regenerative system for a 660 MW supercritical unit running at the IGT-setting mode. Energy 2019;179. <https://doi.org/10.1016/j.energy.2019.05.026>.
- [13] Oyedepo SO, et al. Thermodynamics analysis and performance optimization of a reheat – regenerative steam turbine power plant with feed water heaters. Fuel 2020;280. <https://doi.org/10.1016/j.fuel.2020.118577>.

- [14] A. M. Khoshkar Vandani, F. Joda, F. Ahmadi, and M. H. Ahmadi, "Exergoeconomic effect of adding a new feedwater heater to a steam power plant," *Mech. Ind.*, vol. 18, no. 2, 2017, doi: 10.1051/meca/2016051.
- [15] Kurbanoglu A, Alagoz I, Elmali A. Full repowering of existing fuel-oil fired power plant: modeling and performance evaluation. *Energy Convers Manag* 2022;270. <https://doi.org/10.1016/j.enconman.2022.116288>.
- [16] Bartnik R, Buryn Z, Hnydiuk-Stefan A. Comparative thermodynamic and economic analysis of a conventional gas-steam power plant with a modified gas-steam power plant. *Energy Convers Manag* 2023;293. <https://doi.org/10.1016/j.enconman.2023.117502>.
- [17] Chen X, Zhang C, Chen X, Peng Z, Gao H, Gong X. Performance analysis of a novel biomass gasification system coupled to a coal-fired power plant based on heat and water recovery. *Energy Convers Manag* 2024;299:117822. <https://doi.org/10.1016/j.enconman.2023.117822>.
- [18] S. Nikbakht Naserabad, A. Mehrpanahi, and G. Ahmadi, "Multi-objective optimization of feed-water heater arrangement options in a steam power plant repowering," *J. Clean. Prod.*, vol. 220, 2019, doi: 10.1016/j.jclepro.2019.02.125.
- [19] Liu J, Chen H, Zhao S, Pan P, Wu L, Xu G. Evaluation and improvements on the flexibility and economic performance of a thermal power plant while applying carbon capture, utilization & storage. *Energy Convers Manag* 2023;290. <https://doi.org/10.1016/j.enconman.2023.117219>.
- [20] M. Ameri, P. Ahmadi, and A. Hamidi, "Energy, exergy and exergoeconomic analysis of a steam power plant: A case study," *Int. J. Energy Res.*, vol. 33, no. 5, 2009, doi: 10.1002/er.1495.
- [21] C. Zhang, Y. Wang, C. Zheng, and X. Lou, "Exergy cost analysis of a coal fired power plant based on structural theory of thermoeconomics," *Energy Convers. Manag.*, vol. 47, no. 7–8, 2006, doi: 10.1016/j.enconman.2005.06.014.
- [22] Hao Y, Tan L. Symmetrical and unsymmetrical tip clearances on cavitation performance and radial force of a mixed flow pump as turbine at pump mode. *Renew Energy* 2018;127. <https://doi.org/10.1016/j.renene.2018.04.072>.
- [23] A. Al Jubori, A. Daabo, R. K. Al-Dadah, S. Mahmoud, and A. B. Ennil, "Development of micro-scale axial and radial turbines for low-temperature heat source driven organic Rankine cycle," *Energy Convers. Manag.*, vol. 130, 2016, doi: 10.1016/j.enconman.2016.10.043.
- [24] Liu M, Tan L, Cao S. Theoretical model of energy performance prediction and BEP determination for centrifugal pump as turbine. *Energy* 2019;172. <https://doi.org/10.1016/j.energy.2019.01.162>.
- [25] A. M. Al Jubori, R. K. Al-Dadah, S. Mahmoud, and A. Daabo, "Modelling and parametric analysis of small-scale axial and radial-outflow turbines for Organic Rankine Cycle applications," *Appl. Energy*, vol. 190, 2017, doi: 10.1016/j.apenergy.2016.12.169.
- [26] R. April, "Sky-the-limit-report_Apr21-compressed," no. April, 2021.
- [27] Bouarfa I, El Ydrissi M, El Hafdaoui H, Boujoudar M, Jamil A, Bennouna EG. Developing optical and thermal models with experimental validation of parabolic trough collector for moroccan industrial heat applications. *Sol Energy Mater Sol Cells* 2023;266(November):2024. <https://doi.org/10.1016/j.solmat.2023.112676>.
- [28] Elfeky KE, Wang Q. Techno-economic assessment and optimization of the performance of solar power tower plant in Egypt's climate conditions. *Energy Convers Manag* 2023;280. <https://doi.org/10.1016/j.enconman.2023.116829>.
- [29] G. Ahmadi, D. Toghraie, and O. A. Akbari, "Solar parallel feed water heating repowering of a steam power plant: A case study in Iran," *Renew. Sustain. Energy Rev.*, vol. 77, no. May 2016, pp. 474–485, 2017, doi: 10.1016/j.rser.2017.04.019.
- [30] Baigorri J, Zaversky F, Astrain D. Massive grid-scale energy storage for next-generation concentrated solar power: a review of the potential emerging concepts. *Renew Sustain Energy Rev* 2023;185(August):113633. <https://doi.org/10.1016/j.rser.2023.113633>.
- [31] Ghorbani P, et al. Modeling and thermoeconomic analysis of a 60 MW combined heat and power cycle via feedwater heating compared to a solar power tower. *Sustain Energy Technol Assessments* 2022;54(November). <https://doi.org/10.1016/j.seta.2022.102861>.
- [32] Jamel MS, Abd Rahman A, Shamsuddin AH. Advances in the integration of solar thermal energy with conventional and non-conventional power plants. *Renew Sustain Energy Rev* 2013;20. <https://doi.org/10.1016/j.rser.2012.10.027>.
- [33] Ahadi P, Fakhrabadi F, Pourshaghagh A, Kowsary F. Optimal site selection for a solar power plant in Iran via the analytic hierarchy process (AHP). *Renew Energy* 2023;215. <https://doi.org/10.1016/j.renene.2023.118944>.
- [34] Salehi S. The role of developers in accepting solar energy in Iran: a case study in golestan province. *Sol Energy* 2023;264. <https://doi.org/10.1016/j.soleren.2023.111967>.
- [35] Memarzadeh G, Keynia F. Solar power generation forecasting by a new hybrid cascaded extreme learning method with maximum relevance interaction gain feature selection. *Energy Convers Manag* 2023;298(August). <https://doi.org/10.1016/j.enconman.2023.117763>.
- [36] "Solar resource maps and GIS data for 200+ countries | Solargis." <https://solargis.com/maps-and-gis-data/download/iran> (accessed Jan. 21, 2024).
- [37] "JRC Photovoltaic Geographical Information System (PVGIS) - European Commission." https://re.jrc.ec.europa.eu/pvg_tools/en/tools.html#TMY (accessed Jan. 21, 2024).
- [38] Abdolahinia H, Heidarizadeh M, Rahmati I. Assessing Iran and its neighbors for prospects and challenges: the case of the electrical sector. *Renew Sustain Energy Rev* 2024;193:114190. <https://doi.org/10.1016/j.rser.2023.114190>.
- [39] Matjanov EK, Akhorkhujaeva ZM. Solar repowering existing steam cycle power plants. *Int J Thermofluids* 2023;17(January):100285. <https://doi.org/10.1016/j.ijft.2023.100285>.
- [40] Sumayli H, et al. Integrated CSP-PV hybrid solar power plant for two cities in Saudi Arabia. *Case Stud Therm Eng* 2023;44(February):102835. <https://doi.org/10.1016/j.csite.2023.102835>.
- [41] Alam MI, Nuhash MM, Zihad A, Nakib TH, Ehsan MM. Conventional and emerging CSP technologies and design modifications: research status and recent advancements. *Int J Thermofluids* 2023;20(June):100406. <https://doi.org/10.1016/j.ijft.2023.100406>.
- [42] Settino J, Ferraro V, Morrone P. Energy analysis of novel hybrid solar and natural gas combined cycle plants. *Appl Therm Eng* 2023;230. <https://doi.org/10.1016/j.aplthermeng.2023.120673>.
- [43] Khaleel OJ, Basim Ismail F, Khalil Ibrahim T, bin Abu Hassan SH. Energy and exergy analysis of the steam power plants: a comprehensive review on the classification, development, improvements, and configurations. *Ain Shams Eng J* 2022;13(3):101640. <https://doi.org/10.1016/j.asenj.2021.11.009>.
- [44] Jensen AR, et al. Demonstration of a concentrated solar power and biomass plant for combined heat and power. *Energy Convers Manag* 2022;271(August). <https://doi.org/10.1016/j.enconman.2022.116207>.
- [45] Alotaibi S, Alotaibi F, Ibrahim OM. Solar-assisted steam power plant retrofitted with regenerative system using parabolic trough solar collectors. *Energy Rep* 2020;6:124–33. <https://doi.org/10.1016/j.egyr.2019.12.019>.
- [46] Kabiri S, Khoshgoftar Manesh MH, Yazdi M, Amidpour M. Dynamic and economical procedure for solar parallel feedwater heating repowering of steam power plants. *Appl Therm Eng* 2020;181(July):115970. <https://doi.org/10.1016/j.aplthermeng.2020.115970>.
- [47] Mehrpooya M, Taromi M, Ghorbani B. Thermo-economic assessment and retrofitting of an existing electrical power plant with solar energy under different operational modes and part load conditions. *Energy Rep* 2019;5:1137–50. <https://doi.org/10.1016/j.egyr.2019.07.014>.
- [48] Ahmadi GR, Toghraie D. Energy and exergy analysis of Montazeri steam power plant in Iran. *Renew Sustain Energy Rev* 2016;56:454–63. <https://doi.org/10.1016/j.rser.2015.11.074>.
- [49] Behar O, Khellaf A, Mohammadi K. A novel parabolic trough solar collector model – validation with experimental data and comparison to engineering equation solver (EES). *Energy Convers Manag* 2015;106:268–81. <https://doi.org/10.1016/j.enconman.2015.09.045>.
- [50] James C, Kim TY, Jane R. A review of exergy based optimization and control. *Processes* 2020;8(3):pp. <https://doi.org/10.3390/PR8030364>.
- [51] Li G. Energy and exergy performance assessments for latent heat thermal energy storage systems. *Renew Sustain Energy Rev* 2015;51. <https://doi.org/10.1016/j.rser.2015.06.052>.
- [52] Rosen MA, Dincer I. Exergy as the confluence of energy, environment and sustainable development. *Exergy, An Int J* 2001;1(1):pp. [https://doi.org/10.1016/s1164-0235\(01\)00004-8](https://doi.org/10.1016/s1164-0235(01)00004-8).
- [53] Eke MN, Onyejekwe DC, Illoeje OC, Ezekwe CI, Akpan PU. Energy and exergy evaluation of a 220MW thermal power plant. *Niger J Technol* 2018;37(1). <https://doi.org/10.4314/njt.v37i1.15>.